University of Stavanger

Faculty of Science and Technology

MASTER'S THESIS

Study program/Specialization: Petroleum Engineer/ Drilling and Well Technology	Spring semester, 2021 Open
Writer: Sjur Haugen Bjørlo	
Faculty supervisor: Hans Joakim Skadsem Hermonja A. Rabenjafimanantsoa Rune Wiggo Time	
Thesis title: An Experimental Study of "Heavy over Light" Density-Unstable Displacement of Newtonian Fluids in a Vertical Annular Geometry of Interest to Reverse Circulation Cementing	
Credits (ECTS): 30	
Key words: Rayleigh-Taylor Instability, Reverse Circulation Cementing, Primary Cementing, Kelvin-Helmholtz Instability, Density-Unstable Displacement, Fluid Instabilities, Fluid flow, Atwood number, Froude number, Reynolds number, Concentric and Eccentric Annulus	Pages: 62 + enclosure: 22 Stavanger, 15.06.2021 Date/year

An Experimental Study of "Heavy over Light" Density-Unstable Displacement of Newtonian Fluids in a Vertical Annular Geometry of Interest to Reverse Circulation Cementing

by
Sjur Haugen Bjørlo

Thesis submitted in fulfillment of the requirements for the degree of Master

Faculty of Science and Technology
Department of petroleum Engineering
2021

Abstract

When an oil well is constructed it is important to cement the casing in place. The cement's main objectives is to support the casing and ensure zonal isolation to prevent leakage of reservoir fluids to the surface. Primary cementing is therefore crucial for the well integrity. However, primary is considered a complex operation and needs to be carefully planed. There are different techniques for cementing, but the main goal is the same; place cement in the annuls by safely displacing the drilling fluid. The most common way of displacing is by pumping cement slurry, spacers and washers through the inside of the casing and back up the outside of the casing. However, reverse circulation cementing, is an alternative method, where the cement slurry, spacers and washers are pumped down on the outside of the casing. Reverse circulation cementing has been found to have some advantages while cementing lost circulation- and fragile zones compared to conventional cementing [1]. In contrast to conventional cementing, when preforming reverse circulation cementing the heavier cement slurry is on top of the lighter drilling fluid leading to a density-unstable "heavy over light" displacement. While the displacement mechanisms have been explored in depth for conventional circulation cementing where the denser cement slurry is below and displacing the lighter mud upward, little is still known about the displacement efficiency in reverse circulation cementing with the mechanically unstable configuration of cement slurry above and displacing lighter mud downward.

We will in this study continue Camilla Bjørnsen's work on density-unstable of Newtonian fluid in an annular space. The focus is on different flow velocities and density differences between displacing and displaced fluid. In an experimental setup where colored heavy displacement fluid is separated with a valve above a lighter fluid and ran through a pipe is filmed to study the displacement. The heavy fluid is mixed with NaCl as a weighting agent to achieve various density differences. Further, there is an outlet valve to regulate the flow velocity. Displacement with At of 0.0035, 0.01 and 0.02 was ran with flow velocities of 0 mm/s, 10 mm/s, 20mm/s and 40 mm/s. Mixing, transverse flow and back flow was observed in all the experiments conducted. However, with increasing flow rate the mixing and back flow was reduced. Furthermore, an increase in At resulted in faster settling of heavy fluid but increased the mixing.

Acknowledgement

I would like to express my gratitude to my supervisors at UiS; Associate Professor Hans Joakim Skadsem, Professor Hermonja A. Rabenjafimanantsoa and Professor Rune Wiggo Time. Your guidance and inputs have helped me a lot through out this thesis.

I would also like to thank my student group; PHD student Maryam Ghorbani and Bachelor's student Sveinung Huglen Bratten. All your help and collaboration at the lab has made my days during lab a lot easier and a lot more fun.

Further on i would like to thank my family and friends who have supported and encouraged me through my years as a student. Without you I would not be where i am today.

Last but not least i would like to thank Niels Christensen, the inventor of the O-ring. Without this invention Sveinung and me would probably be trying to close the leak in our flow meter still.

Again thank you all!

Contents

List of Figures

List of Tables

Nomenclature

γ	Shear rate
μ	Viscosity
∇	Vector operator
ρ	Density
ρ_1	Density of heavy fluid
ρ_2	Density of light fluid
τ	Shear stress
At	Atwood number
D	Diameter
D_H	Hydraulic diameter
f_1, f_2	Correction terms
Fr	Froude number
g	Gravitational constant
h	Penetration depth
ID	Inner diameter
KA, KB	Apparatus constants
L	Length
m	Mass
OD	Outer diameter
P, p	Pressure
Q	Flow rate
r_i	Inner radius
r_o	Outer radius
Re	Reynolds number
V	Voltage
V	Volume
v	Flow velocity

Abbreviations

ECD	Equivalent circulation density
HOL	Heavy over light
KHI	Kelvin-Helmholtz instability
RTI	Rayleigh-Taylor instability
RCC	Reverse circulation cementing

Chapter 1

Introduction

1.1 Background

Primary cementing is an important part in drilling a well to ensure well integrity, structural support for casings and prevent leakage with zonal isolation. Leakage of oil or gas into the annulus may result in uncontrolled flows. Uncontrolled flows can lead to many serious problems such as blow outs which can have catastrophic effects on the environment and can even be fatal [2]. Cementing is therefor considered a complex and critical operation in the oil and gas industry. When a well is drilled it is done in different sections due to different formation and pressures as the wellbore gets deeper into the earths crust. After each section is drilled a steel casing is lowered down into the wellbore and its objective is to protect the formation and the wellbore from internal and external forces. After the casing is installed it needs to be cemented in place.

Conventionally a train of cement slurry, spacer and washers are pumped down through the inside of the casing and out into the annulus at the bottom. When the cement is pumped into the annulus it is important to displace the drilling mud in the well in such a manner that the cement slurry do not become contaminated by mixing with the mud or that there is residual drilling mud in the annulus. Contamination of the cement may result in channeling and degraded cement. The displacement of drilling fluid is dependant on rheology, fluid properties and flow rate and drilling fluid may have different properties for different wells. It is therefore important to plan and design cement operation well and understand how different properties affect the displacement to ensure that well integrity is preserved.

An alternative method of cementing, provided there is access to the annulus from the surface, is the reverse circulation cementing (RCC). In RCC the cement slurry, spacer and washers are pumped down through the annulus on the outside of the casing. RCC is an alternative often used when weak formations are present and for potential lost circulation zones [1]. The displacement for RCC compared to conventional cementing is still dependant on rheology, fluid properties and flow rate, however unlike conventional cementing the heavier fluids is on top of the lighter. This leads to an unstable "heavy over light"(HOL) displacement. The HOL leads to instabilities such

as the Rayleigh-Taylor which again may lead to mixing between fluids.

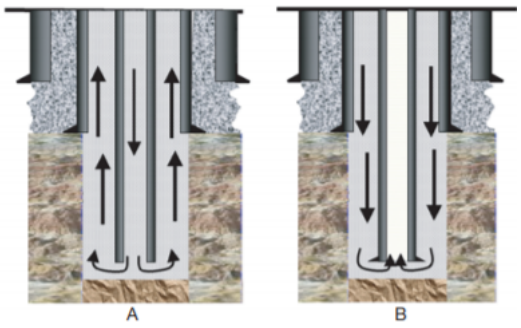

Figure 1.1: A; Conventional cementing technique B; Reverse circulation cementing [1]

1.2 Problem statement and objectives

This thesis is a continuation on the work of former master student Camilla Bjørnsen on HOL displacement in a reverse circulation setup. There is still a knowledge gap around the reverse circulation cementing technique and this thesis aim is to continue Bjørnsen's work and expand on her findings. Further, an optimization of the experimental setup and bring in a clearer dye for better image analysis will be done. The objective of the thesis will be to:

- Expand on Bjørnsen's data by introducing one more Atwood number and flow velocity and study the effect of Atwood number (Density difference) and velocity on displacement
- Improve on experimental setup for better image analysis in MatLab
- Study front velocity

1.3 Limitation

The fluids used in the experiments are Newtonian fluids with constant low viscosity. The fluids are miscible, and the flow is laminar and gravity induced. Further the experimental setup is vertical. In the field it is often non-Newtonian fluids, immiscible fluids such as oil and water. The flow regime might be turbulent and the well bore might have an inclination or even be horizontal. Moreover, the flow is induced by pumping. These cases are not considered in this thesis.

1.4 Approach

The thesis consists of some prior literature study, but consist mostly of experimental results. The experiments and improvements of the experimental setup was done by a team of Bachelor student Sveinung Huglen Bratten, PHD student Maryam Ghorbani and myself.

1.5 Safety and hazards

The experimental rig is 3 meters tall and improvements was done in the height by climbing ladders. It was therefor a fall hazard present while improvements was done. To ensure our safety a safety harness attached to a rigid surface was used whenever work in the height was done. Furthermore, fluids was transported around the lab so it was important to clean up fluid spills from the ground to prevent slip hazard. Due to the ongoing Covid-19 pandemic all equipment and tools used was limited to only the students working on the project. Further, face masks was worn whenever a distance of 2 meter between the students was unachievable.

Chapter 2

Theory

2.1 Wellbore design

When an oil well is drilled it is done in different sections due to different pressure gradients and formations as the borehole goes deeper into the earths crust. A well starts typically off with a 30 inch conductor casing with a borehole of 36 inches, and ends up with a 7 in. production liner with an 8 1/2 in. borehole. The gap between casing and formation, casing and casing, and casing and liner is called an annuls. To prevent leakage of fluids between these sections in the annulus the casing is cemented in place as shown as the gray areas in figure 2.1. This is called primary cementing and the main objective is zonal isolation to prevent migration of fluids up the annulus, protect casing against corrosive fluids and support the casing string [3]. To ensure good zonal isolation and well integrity it is important that the drilling mud is properly displaced [4, p.143]

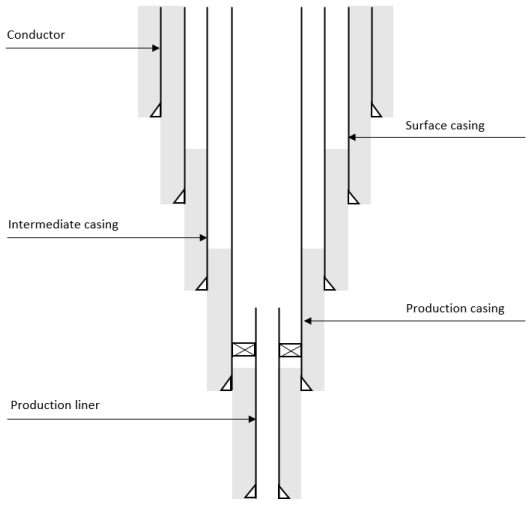

Figure 2.1: Representation of a typical well design

2.1.1 Cement techniques: Conventional vs. Reverse

The most common way to cement a casing in place is the conventional method of pumping cement slurry and spacer fluid through the casing and up the annulus [5]. However, in some cases where for instance important loss circulation zones or fragile formations occur near the casing shoe, reverse circulation cementing may be the only solution [4]. Reverse circulation cementing (RCC) is when cement slurry, washers and spacer fluid is pumped down through the annulus in the opposite direction of normal flow in a well operation. The cementing process may also be done in steps, where the casing is cemented up to a fragile zone with the conventional technique, and then RCC is used above the fragile zone. This is done by bull heading the cement down the annulus to cement the top of the annulus. Figure 2.2 shows a schematic of both revers and conventional cementing.

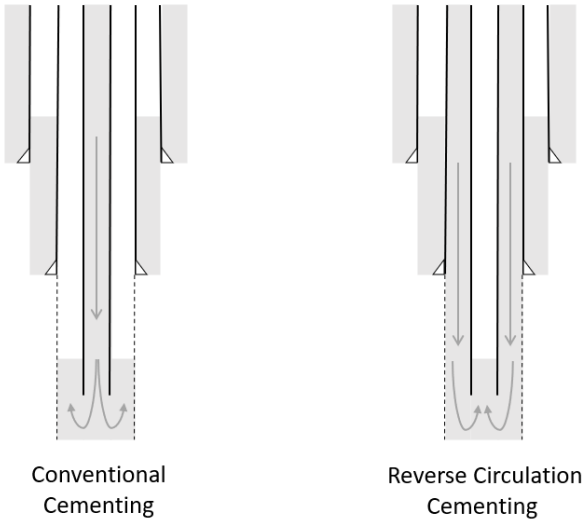

Figure 2.2: Representation of Conventional and reverse circulation cementing

There are both advantages and disadvantages with RCC and there are conducted several studies on the subject. Kuru and Seatter list the following [1]:

Advantages:

- Substantial reduction of equivalent circulation density (ECD)
- Minimize the excess cement needed for a given job
- Gravity assists in cement placing
- Allow cements to set, in spite of high temperature differential
- Reduce placement time of cement
- Customize the setting order of cement
- Allows for customization and reduction of transition times
- Improved safety and environmental management
- Improved productivity due to less risk of cement invasion into the producing zone

Disadvantages:

- Extra design effort
- May need an indicator to know when cement turns the corner
- More iron and special kit needed to rig up for an RCC job
- May require pressure to be held casing as "back pressure"
- Understanding of drilling fluid characteristics is more critical

Moore, Bour, Reed and Hernandez [6] state that one of the major advantages of RCC is that it reduces the frictional and hydrostatic pressure, which can be of great importance when cementing in fragile formations. Furthermore Griffith, Nix, and Boe [7] argues that by lowering the ECD the formation can support a higher cement column.

2.1.2 Concentric and Eccentric wells

The importance of pipe centralization has been recognised since the first cementing studies where published back in 1940 [5, p.95]. In a eccentric annulus the casing is not in the middle of the borehole contrary to a concentric annulus. Eccentricity or standoff is often measured in percentage where a 100% stand off means the casing is perfectly centralized and 0% is where the

casing touches the borehole wall, figure 2.3 shows different representations of eccentricities.

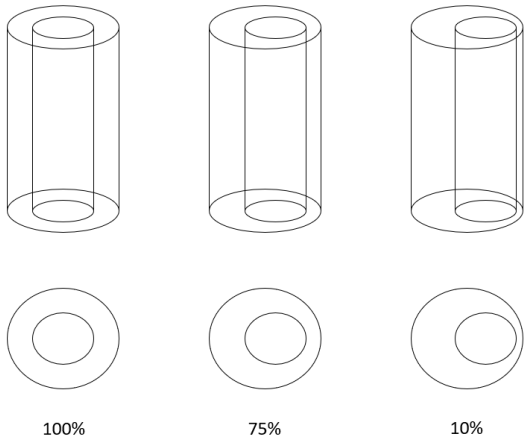

Figure 2.3: Schematic of eccentricity in a well

In an eccentric annuls the flow tends to follow the path of least resistance and displace on the wider side of the annulus. This may lead to an uneven distribution of cement along the casing as shown in figure 2.4

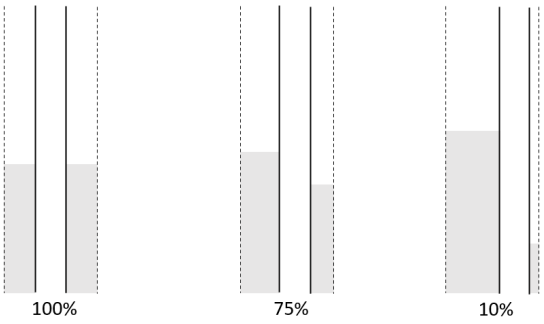

Figure 2.4: Effect of different eccentricities on cement

2.2 Fluid properties

2.2.1 Density

Density (ρ) is a measurement of mass (m) per unit volume (V). Fluids with the same volume, but different mass will have different densities. Larger density of a fluid will resort in a "heavier" fluid. A heavy fluid will displace a "lighter" fluid due to gravity, therefore the density is an important fluid property when it comes to displacement. The density is given by:

$$\rho = \frac{m}{V} \tag{2.1}$$

The density of a fluid is dependent on fluid content and temperature. For instance water has different density at different temperatures where at 4°C water has the largest density. Furthermore the salinity of water plays an effect on the density. In a cement operation the density of cement is usually the largest followed by spacer fluid and drilling mud has the lowest density.

2.2.2 Viscosity

The viscosity describes the internal friction of a moving fluid. It is the resistance of a fluid to deform, or to flow. [8] A fluid with low viscosity will flow more easily than a fluid with high viscosity. This is because a low viscosity fluid's molecular makeup results in a very low friction when flowing. Viscosity (μ) is defined by shear stress (τ) and shear rate (γ) described in equation 2.2

$$\mu = \frac{\tau}{\gamma} \tag{2.2}$$

2.3 Flow

Fluid flow is an important part of the displacement in cementing. The nature of the flow, if it is steady or unsteady, and the flow pattern affects the displacement.

2.3.1 Natural vs. forced flow

Fluid flow that is induced by natural causes such as gravity and/or internal causes, for instance buoyancy, is called natural flow. In the case of the "Heavy over Light"experiment the natural flow is what drives the fluid.

Gravity forces the fluid down and out of the pipe, and since there is a density difference between the fluids with heavy on top buoyancy plays an effect. Furthermore, since the fluid on top is heavier than the one below, gravity affects it more and it will penetrate the lighter fluid. Forced flow is where an external force acts on the fluid. An external force may be a pump or a fan, and in cementing operations a pump is used to drive the flow.

2.3.2 Steady and unsteady state flow

For a steady state flow, parameters such as velocity, pressure and density at a point in the system is independent of time. Unsteady flow on the other hand may have changes in mass or pressure with respect to time. For the cementing process the flow is unsteady since the interface between the fluids changes with time. However, the displacement is steady if the interface is fixated and moves with the bulk velocity of the flow.

In the industry, a steady displacement of drilling mud by cement is desired to get a continuous and complete displacement around the annulus [9].

2.4 Dimensionless numbers and scaling

2.4.1 Scaling

In physical studies, there is often a desire to obtain a relationship between quantities that characterize the phenomenon being studied [10]. Also a physical similarity of an experiment setup to the real life event being looked at is important i.e. the annulus in a well bore and the experiment has somewhat the same geometry. Dimensionless numbers are often used in scaling to see similarities with experiments and real life situation without the need to convert or scale dimensions.

2.4.2 Reynolds number

Reynolds number (Re) expresses the ratio between inertial force and viscous forces. [11] Re is a dimensionless number and describes the flow regime.

For flow in a pipe the Reynolds number is defined as:

$$Re = \frac{\rho v D_H}{\mu} \tag{2.3}$$

where ρ is the density, v is fluid velocity, D_H is hydraulic diameter of the pipe, and μ is the viscosity. For an annular pipe D_H becomes:

$$D_H = D_{outer} - D_{inner} \tag{2.4}$$

When viscous forces are larger relative to inertial forces, the flow tends to become laminar. In laminar flow layers of fluid is running side by side with different speeds and almost no mixing between the layers [12]. In turbulent flow on the other hand the inertial forces are more dominant and the flow is more chaotic. Here there is more mixing. Figure 2.5 illustrates the different flow regimes and table 2.1 shows the different limits of Reynolds number where the flow behaves laminar, transient or turbulent.

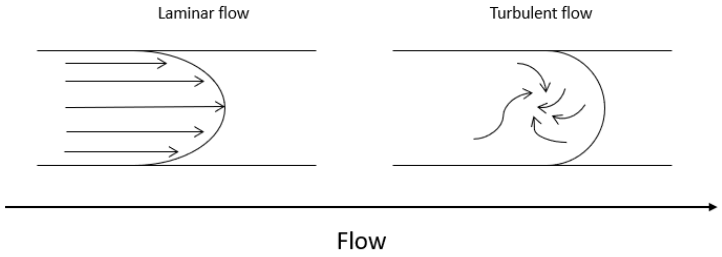

Figure 2.5: Schematic of Laminar and Turbulent flow

Table 2.1: Flow regime classification

$\text{Re} \leq 2300$	Laminar flow regime
$2300 \leq \text{Re} \leq 4000$	Transient flow regime
$\text{Re} \geq 4000$	Turbulent flow regime

2.4.3 Atwood number

Atwood number (At) is a dimensionless density difference between two fluids. In an unstable heavy over light arrangement, the density relation between heavy and light fluid is important for the displacement. Atwood number is described by:

$$At = \frac{\rho_1 - \rho_2}{\rho_1 + \rho_2} \tag{2.5}$$

Where $\rho_1 > \rho_2$. The Atwood number is an important parameter in instabilities like Rayleigh-Taylor.

2.4.4 Froude number

Froude is a dimensionless ratio between flow inertia and an external field. It is based on the speed length ratio and defined by:

$$Fr = \frac{v}{\sqrt{gD}} \tag{2.6}$$

where v is fluid velocity, g is gravitation and D is a characteristic length.

Densimetric Froude number can be obtained by considering the Boussineq approximation:

$$Fr = \frac{v}{\sqrt{AtgD}} \tag{2.7}$$

where At is the Atwood number.

2.5 Fluid instability

2.5.1 Rayleigh-Taylor instability

The interface between two fluids with different densities is unstable if the heavier fluid is located above the lighter fluid and accelerated with gravity. This instability is called the Rayleigh-Taylor instability (RTI) [13]. Another part of the instability is the buoyancy effect of the lighter fluid driving it up towards the denser fluid. The RTI leads to a turbulent mixing between the two fluids where the lighter fluid rises up into the denser fluid and the denser fluid will sink into the lighter fluid and penetrate it. The rise of lighter fluids is called bubbles and the penetration from heavier fluid is called spikes. Figure 2.6 shows two planar laser induced fluorescence images of water at different temperatures mixing. There is a flow from left to right and the top layer is water at 17 °C while the lower layer is water at 22 °C. Since water expands with temperature the density gets lower with increasing temperature and there is a small density difference. At figure 2.6(a) the mixing is at an early stage and a two-dimensional single-wavelength perturbation is starting to grow downstream. Figure 2.6(b) is at a much later stage of mixing and a mushroom like structure can be seen where "black" lighter fluid is fully trapped inside the "white" heavier fluid. This mushroom structure is typical for RT mixing [14].

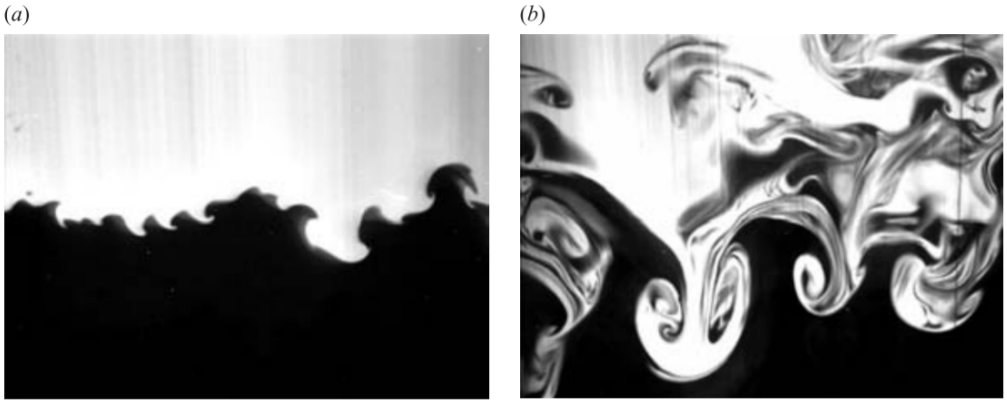

Figure 2.6: Planar laser induced fluorescence images of evolution of RTI. (a) shows RTI at an early stage and (b) at late times in evolution. [14]

RTI develops in different stages. The first stage there is an exponential growth of perturbation with time and the growth can be analysed using linearized form of the dynamical equations for the fluid. This is shown in the first image of figure 2.7. In the next stage the instability saturates and perturbation speed grows at a constant rate. Lastly longer wavelengths overtake due to their continued growth [14] [15].

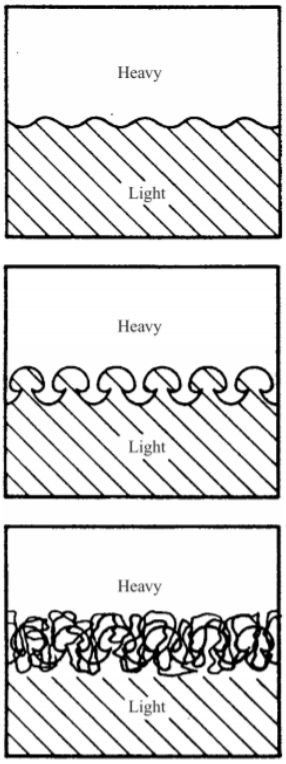

Figure 2.7: The Different stages of RTI [14]

The depth of which the turbulent mixing zone penetrates the denser fluid has a quadratic growth with time and is given by:

$$h = \alpha Atgt^2 \tag{2.8}$$

Where At is the Atwood number, g is gravitational acceleration, t is time and α is a constant. It has been shown experimentally that α is approximately 0.06. [16]

2.5.2 Kelvin-Helmholtz instability

The Kelvin-Helmholtz instability (KHI) is a fluid instability that typically occurs in parallel shear flows, where small scale perturbation draw kinetic energy from the average flow [17]. KHI is a common phenomena in for instance clouds as shown in figure 2.8. Due to difference in velocity, like shear flows, vorticity occurs at the interface. This results in an unstable vortex sheet that rolls up in a spiral at the interface. KHI results in a turbulent flow that increases mixing between fluids.

Figure 2.8: Kelvin-Helmholtz instability in clouds [18]

2.6 Fluid transport and flow governing equations

The following fundamental laws can be used to derive fluid governing equations [19]:

- Conservation of mass
- Conservation of liner momentum (Newton's 2nd law)
- Conservation of energy (1st law of thermodynamics)

Conservation of mass is described in the continuity equation while conservation of liner momentum is described by the Navier-Stokes equations. These physical principals are used to solve fluid flow numerically in computational fluid dynamics (CFD).

2.6.1 Continuity equation

The continuity equation is based on the physical principle that mass is conserved. It describes movement or transport of a given quantity. The equation states that local increase of density with time must be balanced by a divergence of mass flux [20].

$$\frac{\partial \rho}{\partial t} + \nabla \cdot (\rho \vec{u}) = 0 \tag{2.9}$$

Where ρ is the density, t is time and $\vec{u}$ is the flow velocity vector.

For an incompressible fluid where density is constant the continuity equation can be reduced to:

$$\nabla \cdot \vec{u} = 0 \tag{2.10}$$

2.6.2 Navier-Stokes equations

The Navier-Stokes equation uses Newton's 2nd law to describe the motion of viscous fluids. For a Newtonian and incompressible fluid the Navier-stokes equation becomes:

$$\underbrace{\rho\left(\frac{\partial \vec{u}}{\partial t} + (\vec{u}\cdot\nabla)\vec{u}\right)}_{(1)} = -\underbrace{\nabla p}_{(2)} + \underbrace{\mu\cdot\nabla^2\vec{u}}_{(3)} + \underbrace{\rho\vec{g}}_{(4)} \tag{2.11}$$

The first part of the equation (1) is the inertial forces, (2) is the pressure forces, (3) is viscous forces and (4) is external forces[21]. In this case the external forces is the hydrostatic pressure.

2.6.3 Navier-Stokes with dimensionless numbers

The Navier-stokes equation can be rearranged to fit different dimensionless numbers for instance; Re, At and Fr. By looking at density (ρ) as an average between a mix of heavy and light fluid it may be written as:

$$\rho_i = \overline{\rho}(1 + \Phi_i At) \tag{2.12}$$

where the subscript i is whether it is heavy or light fluid, Φ_i is +1 for heavy fluid ($i = 1$) and -1 for light ($i = 2$), and $\overline{\rho}$ is the average density of heavy and light fluid:

$$\overline{\rho} = \frac{1}{2}(\rho_1 + \rho_2) \tag{2.13}$$

Furthermore the characteristic velocity scale U_0 such that $\vec{u} = U_0\hat{\vec{u}}$ where $\hat{\vec{u}}$ is an dimensionless velocity vector, and characteristic length scale D_0 such that $x = D_0\hat{x}$ are introduced. The timescale then becomes D_0/U_0 and the Navier stokes equation may be written as:

$$\overline{\rho}(1+\Phi_i At)\frac{U_0^2}{D_0}\left(\frac{\partial \vec{u}}{\partial t} + (\vec{u}\cdot\nabla)\vec{u}\right) = -\frac{p_0}{D_0}\nabla p + \frac{\mu U_0}{D_0^2}\nabla^2 u + \overline{\rho}(1+\Phi_i At)\vec{g} \tag{2.14}$$

where p_0 is a pressure scale. By rearranging equation 2.14 we get:

$$(1 + \Phi_i At)\underbrace{\frac{\overline{\rho}U_0 D_0}{\mu}}_{=Re}\left(\frac{\partial \vec{u}}{\partial t} + (\vec{u}\cdot\nabla)\vec{u}\right) = -\frac{p_0 D_0}{\mu U_0}\nabla p + \nabla^2 u + (1 + \Phi_i At)\frac{\overline{\rho}\vec{g}D_0^2}{\mu U_0} \tag{2.15}$$

Moreover the constant pressure term $\frac{\overline{\rho}\vec{g}D_0^2}{\mu U_0}$ may be absorbed into p:

$$-\frac{p_0 D_0}{\mu U_0}\nabla p + \frac{\overline{\rho}\vec{g}D_0^2}{\mu U_0} \rightarrow -\nabla p' \tag{2.16}$$

where $p_0 = \frac{\mu_0 U_0}{D_0}$ as a pressure scale and let p become $p' + \frac{1}{p_0}\overline{\rho}\vec{g}\cdot\vec{x}$
Now Navier-Stokes becomes:

$$(1+\Phi_i At)Re\left(\frac{\partial\vec{u}}{\partial t} + (\vec{u}\cdot\nabla)\vec{u}\right) = -\nabla p' + \nabla^2\vec{u} + \Phi_i\frac{At\overline{\rho}\vec{g}D_0^2}{\mu U_0} \tag{2.17}$$

The last term in equation 2.17 can be written as:

$$\underbrace{\frac{AtgD_0}{U_0^2}}_{=\frac{1}{Fr^2}} \times \underbrace{\frac{\overline{\rho}U_0 D_0}{\mu}}_{=Re} \cdot \underbrace{\vec{e_g}}_{unitvector for gravity} \tag{2.18}$$

Finally the Navier-Stokes equation becomes:

$$(1+\Phi_i At)Re\left(\frac{\partial\vec{u}}{\partial t} + (\vec{u}\cdot\nabla)\vec{u}\right) = \nabla p' + \nabla^2\vec{u} + \Phi_i\frac{Re}{Fr^2}\vec{e_g} \tag{2.19}$$

The dimensionless numbers that govern flow are At, Re and Fr. Also eccentricity and boundary conditions play a part in the flow [22].

Chapter 3

Methodology

3.1 Experimental Setup

The experimental setup was inherited by a previous Master thesis and made some improvements to. Figure 3.1 shows the experimental setup before the improvements. The improvements made includes changing a damaged hose and adding curtains and a LED-strip for better lighting while filming the experiment.

The setup consist of a 3.09 meter tall vertical transparent acrylic pipe. The pipe has an inner diameter of 50mm and a outer diameter of 60mm. Inside there is a smaller pipe installed from the bottom with a height of 1.96m, with an outer diameter of 32mm making an annular gap of 18mm. Above the inner pipe there is a ball valve separating the upper part of the pipe from the lower part that contains the inner pipe. The upper part is approximately 1m and is used to contain the heavier displacement fluid. Below the ball valve a honeycomb flow straightener is placed to eliminate the effect of valve handling. At the bottom of the rig a tube leading flow out to a drain is connected with an outlet valve. The outlet valve is a 1/4 inch ball valve and is used to control the flow velocity. Attached to the outlet valve is a protractor to measure the angel of valve opening and compare it to flow rate. An electromagnetic flow meter is attached to the outlet tube and at the bottom of the pipe a pressure sensor, both connected to a nearby computer using Pasco software to monitor pressure and flow velocity. A tank acting as reservoir for heavy fluid is placed beside the rig with a bilge pump filling up the upper part of the pipe. The pump ensures that the level of fluid does not drop while a 45°Y-coupling on the top redirects excess fluid back to the tank such that the fluid column height stays the same even though fluid is let out at the outlet valve.

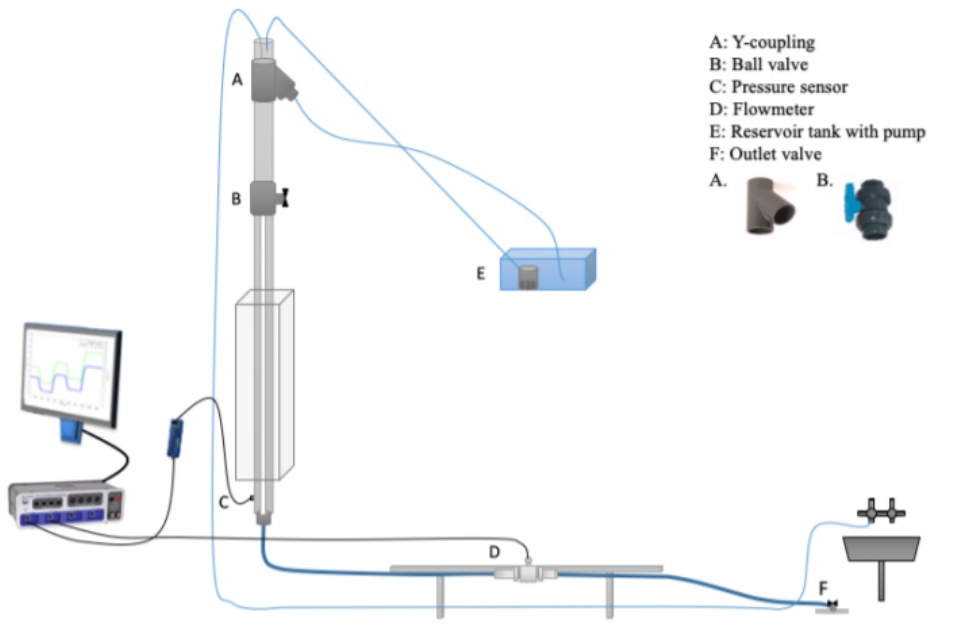

Figure 3.1: Experimental setup. [23, p.24]

3.1.1 Scaling

The scaling of the setup was done by earlier master student C. Bjørnsen. To decide the diameters of the inner and outer pipe she looked at the relation between hole size and casing size in an oil well (see table 3.1). In a 17 1/2 inch hole with a 13 3/8 inch casing the relation is 1.31, while a 12 1/4 inch hole with a 9 5/8 inch casing the relation is 1.27. These are typical annuli in an oil well. For the experiment the inner diameter of the cylinder is 50mm and the outer diameter for the inner pipe is 32mm. This gives a ratio of 1.56 which is slightly larger than in a typical oil well. The higher relation was chosen to better visualize the displacement. The length of the pipe was chosen based on the relation between axial length and hydraulic diameter and circumference. The relations are shown in table 3.2. These should be sufficient enough to see dominating effects of the displacement [23].

Table 3.1: Relation between experimental and oil well annuls [23]

Hole section OD	Inner casing ID	Ratio
In a typical oil well		
17 1/2"	13 3/8"	1.31
12 1/4"	9 5/8"	1.27
8 1/2"	7"	1.21
On experimental setup		
50 mm	32mm	1.56

Table 3.2: Geometrical parameters for experimental setup [23]

Parameter	Symbol	Value
Inner diameter of cylinder (Outer diameter of annulus)	OD	50mm
Outer diameter of inner pipe (Inner diameter of annulus)	ID	32mm
Hydraulic diameter	D_H	18mm
Circumference of annulus	C = $\pi(r_o+r_i)$	128.8mm
Total height of cylinder		3.09m
Height up to ball valve (pipe with annulus)	L	1.96m
Height above ball valve		0.96m
Axial length/hydraulic diameter	L/D_H	109
Axial length/circumference	L/C	15.2

3.1.2 Camera setup

A Nikon D5500 Single-lens reflex digital camera is used to capture the displacement of fluid. The camera is mounted on a ladder next to the rig and films with a frame rate of 60fps. To optimize the video quality a fish tank filled with water is installed around the area of interest due to the circular ends of the pipe. A mirror is setup with an angle next to the pipe to capture the fluid flow on the side of the pipe.

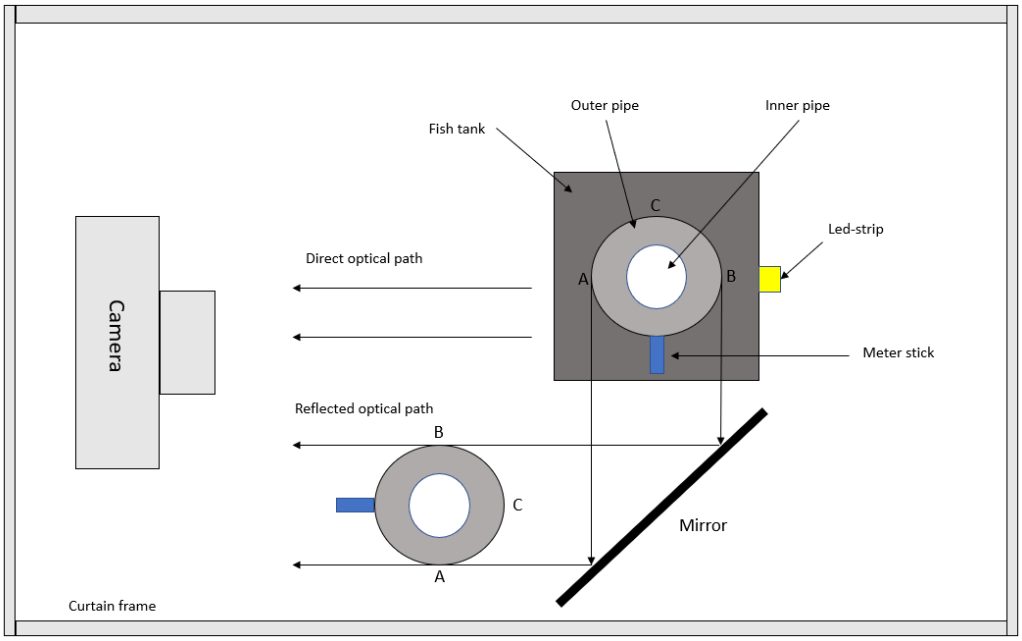

Figure 3.2: Camera setup

Behind the area of interest a white cardboard plate is set up to improve the natural background. Furthermore a LED-light strip has been installed behind the pipe to increase lighting. There has also been installed light blocking curtains around and above the camera and the pipe to block out light from other sources.

3.1.3 PASCO instruments

As mentioned earlier the pressure sensor and the flow meter is connected to Pasco capture software on a computer. Pasco 850 interface is used to connect the sensors to the computer. The pressure sensor is attached to the bottom of the vertical pipe shown at point C in figure 3.1 , while the flow meter is attached to the outlet hose at point D. An example of the Pasco measurements is shown in appendix D.

Pressure sensor

For this experiment an absolute pressure sensor was attached with a VWR silicon tube connecting the pressure sensor nipple to the Pasco interface.

Flow meter

The flow meter used in this experiment is an Endress+Hauser 53. The flow meter is electromagnetic and uses Faraday's law to convert flow into an electric signal. Two field coils are located inside the flow meter setting up a magnetic field perpendicular to the flow across the cross section of the pipe. Furthermore two electrodes are installed at a right angle in the walls of the flow meter to pick up electrical voltage. When a conductive fluid runs through the magnetic field the charged particles in the fluid are separated and forms an electrical voltage. The voltage is proportional with flow velocity [24].

Both the flow meter and pressure sensor has been calibrated (see Appendix A).

3.1.4 Heavy fluid

To achieve a fluid with a higher density than water, salt (NaCl) was added to distilled water. Water can be considered an incompressible Newtonian fluid with constant viscosity and the salt will dissolve in water. Salt as a weighting agent will not affect the other properties than density in a considerable manner. The light fluid in this experiment is fresh water. To distinct the heavy fluid from the light, ink was added to the heavy fluid mixture.

3.1.5 Density meter

A DMA 4100 M density meter was used to determine the density of heavy and light fluid. A sample of the fluid is inserted into a U-tube in the density meter. The U-tube is of borosilicate glass and is being excited to vibrate at its characteristic frequency which changes depending on the density of the sample. "The density is calculated from the quotient of the period of oscillations of the U-tube and the reference oscillator" [25, p.13]

$$\rho = KA \cdot Q^2 \cdot f_1 - KB \cdot f_2 \tag{3.1}$$

Where KA and KB are apparatus constants, Q is quotient of the period of oscillation of the U-tube divided by the period of oscillation of the reference oscillator, and f_1 and f_2 are correction terms for temperature, viscosity and non linearity.

It is important that there are no air bubbles in the U-tube while the density is measured for a correct measuring, therefore the U-tube is shown on a display to ensure only liquid is filled. In addition the U-tube is cleaned between every sample to make sure there are no left over fluid. The glass

tube is flushed with distilled water and cleaned with Acetone. After the cleaning an air pump is inserted in the tube opening to dry it up.

Figure 3.3: DMA 4100 M density meter [25, p.16]

3.2 Experimental Procedure

The pipe is filled with freshwater from a hose, connected from the top of the rig to a water tap, all the way up to the ball valve. To ensure that there is no air trapped in the rig the outlet valve is opened to let air out. After all the air is released the rig is filled up to the ball valve and the ball valve is closed. Pre-made heavy fluid mix is pumped into the upper part of the pipe above the ball valve from the tank. The camera is started to record the displacement and Pasco to measure flow and pressure. After recording is started the ball valve and outlet valve is opened simultaneously. It is important to match outlet valve opening to flow meter voltage such that correct flow velocity is acquired. The pump runs while fluid is let out of the rig to keep the hydrostatic pressure the same throughout the experiment by keeping liquid height constant. After all the light fluid is displaced recording is stopped and the fluid let out of the rig. To ensure there is no leftover salt or ink the rig is cleaned by running water a couple of times through the rig before starting a new run.

3.2.1 Experimental plan

The experimental plan is presented in table 3.3. The light fluid is kept constant while the density of heavy fluid changes. All densities are mixed and ran with no flow and then three different velocities before moving on to the next density. To ensure good results and less uncertainties all experiments will be done three times with the same parameters.

Table 3.3: Fluid selection and parameter chosen for experiments

Series	**Density of displacing fluid** (kg/m^3)	**Density of displaced fluid** (kg/m^3)	**Atwood number**	**Velocity** (mm/s)
1	1005.3	998.3	0.0035	0, 10, 20, 40
2	1018.5	998.3	0.01	0, 10, 20, 40
3	1039.0	998.3	0.02	0, 10, 20, 40

Chapter 4

Results and discussions

4.1 Experimental parameters

The parameters in this experiment that was altered between runs was density of heavy fluid resulting in different Atwood numbers and flow velocity resulting in different Reynolds numbers. The Froude number is dependant on both flow velocity and Atwood number. Table 4.1 shows the different velocities, At, Re, Fr and the ratio between Re and Fr for each run. As seen from the table there are three runs with fairly similar velocity and At, but they vary a little bit. The velocity was especially difficult to get similar for every run since the outlet valve was opened manually and small differences in valve openings resulted in larger difference in velocity. It is desirable to have the same velocity for each run, but this was next to impossible in practice. However the velocities are fairly similar and should be sufficient.

Further the Atwood numbers differs somewhat between runs too. This is because salt was measured and mixed with distilled water and ink, then the density was measured in the density meter. Small differences in the amount of salt or distilled water has an affect on the density. Still the difference is not of a substantial amount and the Atwood numbers should be sufficient for this experiment.

The velocities where found by the use of the flow meter explained in chapter 3.1.3. The flow meter gave a voltage and by calibration (see A.1) the relation between flow rate, Q (ml/s), and voltage, V (V), was found to be:

$$Q = 70.055V - 75.812 \tag{4.1}$$

The flow rate was converted to flow velocity, v (mm/s), by dividing the flow rate by the area, A (mm^2):

$$v = \frac{Q}{A} = \frac{Q}{\pi/4(OD^2 - ID^2)} \tag{4.2}$$

4.1 Experimental parameters

Table 4.1: Overview of experimental parameters for each run

Series	Flow rate (mm/s)	At	Re	Fr	Re/Fr
1.0.1	-	0.00394	-	-	-
1.0.2	-	0.00394	-	-	-
1.0.3	-	0.00394	-	-	-
1.1.1	10.4	0.00354	187	0.415	450
1.1.2	9.44	0.00354	170	0.377	450
1.1.3	9.62	0.00354	173	0.385	450
1.2.1	18.0	0.00349	323	0.723	447
1.2.2	18.5	0.00349	334	0.746	447
1.2.3	19.5	0.00349	351	0.784	447
1.3.1	34.7	0.00349	625	1.40	447
1.3.2	35.5	0.00349	640	1.43	447
1.3.3	34.8	0.00354	627	1.39	447
2.0.1	-	0.0101	-	-	-
2.0.2	-	0.0101	-	-	-
2.0.3	-	0.0101	-	-	-
2.1.1	9.29	0.0103	168	0.218	773
2.1.2	9.90	0.0103	180	0.232	773
2.1.3	10.0	0.0103	181	0.234	773
2.2.1	25.3	0.0103	458	0.592	773
2.2.2	21.6	0.0103	391	0.506	773
2.2.3	21.9	0.0103	396	0.512	773
2.3.1	44.1	0.0103	799	1.03	773
2.3.2	39.8	0.0103	721	0.932	773
2.3.3	37.6	0.0103	682	0.881	773
3.0.1	-	0.0197	-	-	-
3.0.2	-	0.0197	-	-	-
3.0.3	-	0.0197	-	-	-
3.1.1	10.4	0.0198	191	0.176	1082
3.1.2	10.4	0.0198	190	0.176	1082
3.1.3	10.7	0.0198	195	0.180	1082

3.2.1	22.0	0.0199	402	0.371	1085
3.2.2	22.1	0.0199	404	0.372	1085
3.2.3	19.6	0.0199	359	0.330	1085
3.3.1	40.6	0.0199	743	0.684	1085
3.3.2	41.7	0.0199	764	0.704	1085
3.3.3	40.5	0.0199	741	0.682	1085

4.2 Uncertainties

As mentioned there are some difference in velocity and Atwood number between the runs due to human error. Further, the ball valve and outlet valve was manually opened by one person at the ball valve and one at the outlet valve simultaneously. This is difficult to get exactly the same each time and there might be some small differences in valve opening leading to difference in mixing and flow at the start, but these differences should be quite small and it is reasonable to neglect and there is also a honeycomb flow straightener after the ball valve that would reduce this effect. Another uncertainty is the velocity build up. When the outlet valve is opened it takes some time from the opening until the voltage on the Pasco software updates and small adjustments on the valve opening must be done if opening is too large or too small. The velocities recorded in table 4.1 is the average velocity from valve opening until all the light fluid in the area of interest is displaced.
Moreover, it was discovered after all the experiments, when the result was looked at, that the inner pipe is not a 100% concentric. The pipe was intended to be concentric and not eccentric, but there is some eccentricity which is difficult to measure. This will affect the flow somewhat and there seems to be a helical spin on the flow in some of the runs which is suspected to come from the eccentricity.
After each run the rig was flushed with fresh water to clean out the pipes, but there might have been residual salt left in the pipe that would have an effect on the density of the light fluid. However the amount of leftover salt is assumed to be very low after cleaning and will not have a substantial affect on the density difference.

4.3 Visualization of displacement

Figure 4.1 shows the view of the area of interest in the experimental setup from the camera. There are curtains around the setup blocking out external light and (c) shows a LED-strip illuminating the pipe. This LED strip is placed behind the pipe such that the light does not go directly into the camera, and the (c) shows it from the mirror. The black markings in the mirror shown by (g) is drawn on the backside of the fish tank at every 4cm such that one can follow the flow in the mirror. The mirror image is at a different angle and distance to the camera compared to the "real" image and will therefor be compressed. The black markings on the fish tank allows for a comparison between the mirror image and the "real" image. Furthermore, the mirror allows for side view of the backside of the annulus that would not have been seen without it, (e). There is a small blind spot on the left backside, but most of the flow is captured by the camera.

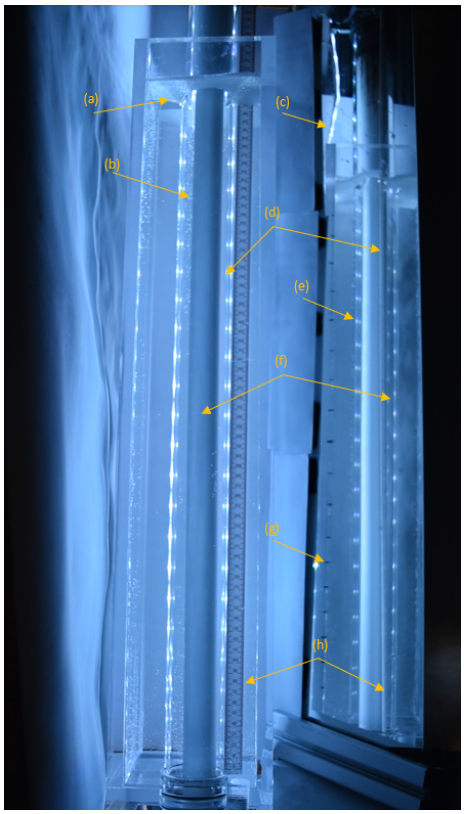

Figure 4.1: Explanation of visualization of the displacement. (a) Styrofoam plates to reduce dust and particles in fish tank, (b) left side of annulus (an.), (c) LED-strip for illumination, (d) right side of an., (e) backside of an., (f) front side of an., (g) black indicators on mirror for every 4cm, (h) meter stick.

The camera used to capture the displacement films with a frame rate of 60fps. To analyse the displacement windows video editor was used, also the videos was split into images using a MatLab script (see C.1). Furthermore, a MatLab script to analyse the displacement front from the split videos was made by Professor Rune W. Time. The script is based on brightness difference in the image pixels where low brightness (from black dye) indicates heavy fluid, and high brightness (from LED-lights) indicates the light fluid. However this was proven too time consuming as every run needed to be fitted differently since the camera is not mounted exactly the same each time and was only done for one run, run 3.3.3 (see C.2).

4.4 Displacement time

The time for the area of interest in the experiments to become fully displaced was recorded and compared for the different Atwood numbers. The time required to fully displace the annulus is the time from the black heavy fluid is seen entering from the ball valve, until only black fluid is seen from the camera. However, there are some uncertainties, such as a small blind spot on the backside of the annulus where there might be some light fluid and if the fluids have mixed, and the analysis is a "rough" approximation. In figure 4.2 median required time for displacement is plotted vs At for the different flow velocities. The diamond shaped points on the graph is the time above the median and the "-" is the time below. The displacement time goes down as At increases, especially for the lower flow velocities.

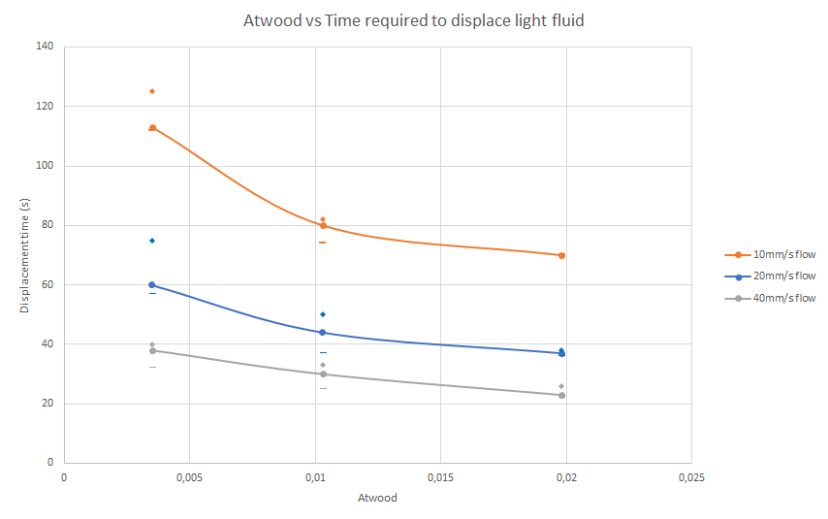

Figure 4.2: Time required for displacement vs Atwood number

4.4 Displacement time

However it is worth noting that, as seen in table 4.1, there are some variation in velocity for the different runs. Moreover, the fluids used are miscible so some mixing between the fluid might occur. Figure 4.3 shows how much volume that exits out of the flow loop from the outlet valve for each of the At. The volume is based on the average for the three runs at each velocity and At and is calculated by multiplying the flow rate (ml/s) by the time required to displace. The black line is the annular volume of the area of interest (V=1159.25 ml). For the light fluid to be completely displaced the volume exiting the flow loop needs to be larger than the annular volume of the area of interest. However, due to mixing the area of interest looks to be completely black although the volume that has exited the flow loop is lower than the volume of the annular space. This means that the displacement times in figure 4.2 not necessarily are completely accurate. Nevertheless the graph might be used to see a trend of increasing the At will decrease the time for required to displace light fluid. For a higher At the volume that exits the flow loop decreases. At At=0.02 the volume exiting is below the black line for all flow velocities which indicates the amount of mixing increases as the At increases. Furthermore, it is seen that with decreasing flow velocity the volume leaving the flow loop decreases. This is most likely due to the time required for displacement is much higher than for higher velocities and the fluids have more time to mix.

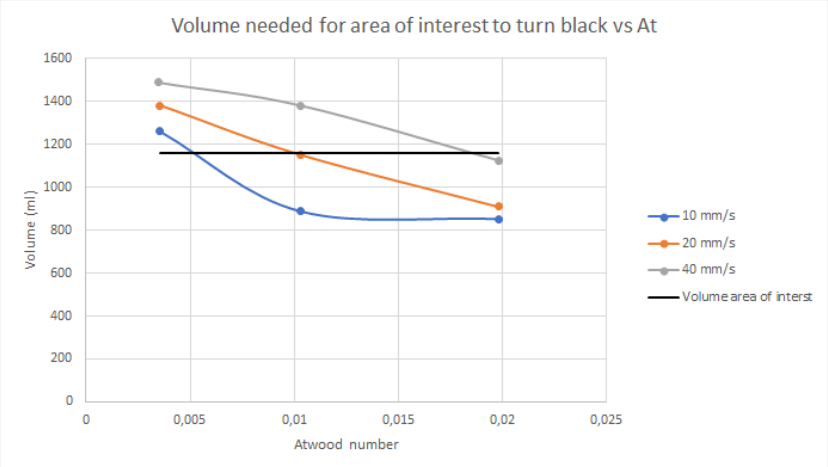

Figure 4.3: Volume leaving flow loop before area of interest is displaced

4.5 Effect of Atwood number

In this section the effect of density difference between the heavy fluid displacing and the light fluid that is being displaced is studied, and what effect the Atwood number has on the displacement. By comparing the displacements with different At and keeping the flow rate constant we can study the effect of At.

4.5.1 No outlet flow

In these series the outlet valve was closed such that there was no flow out of the rig. The only flow is the exchange flow between the two fluids. Since there is no flow the RTI is dominant in the system. Figure 4.4- 4.8 shows series 1.0.1, 2.0.1 and 3.0.2 at different time in the displacement. At the start of the displacement fingering is observed from the heavy fluid entering the annulus before a more constant flow of heavy fluid flow throughout the annulus follows behind the fingers. Moreover, back flow (shown in figure 4.5a) of light fluid traveling upwards in the opposite direction of heavy fluid is observed. There is also some transverse flow as shown in figure 4.6a. The displacing fluid with the highest At, (c), settles at a higher rate than the fluids with lower At, (a) and (b). It seems to be more back flow in the start of the higher At numbers leading to more mixing, but it settles in a shorter time such that the total mixing over time seems less. The concentration of the black fluid at t=240s is darker in figure 4.8 for the At=0,0197.

4.5 Effect of Atwood number

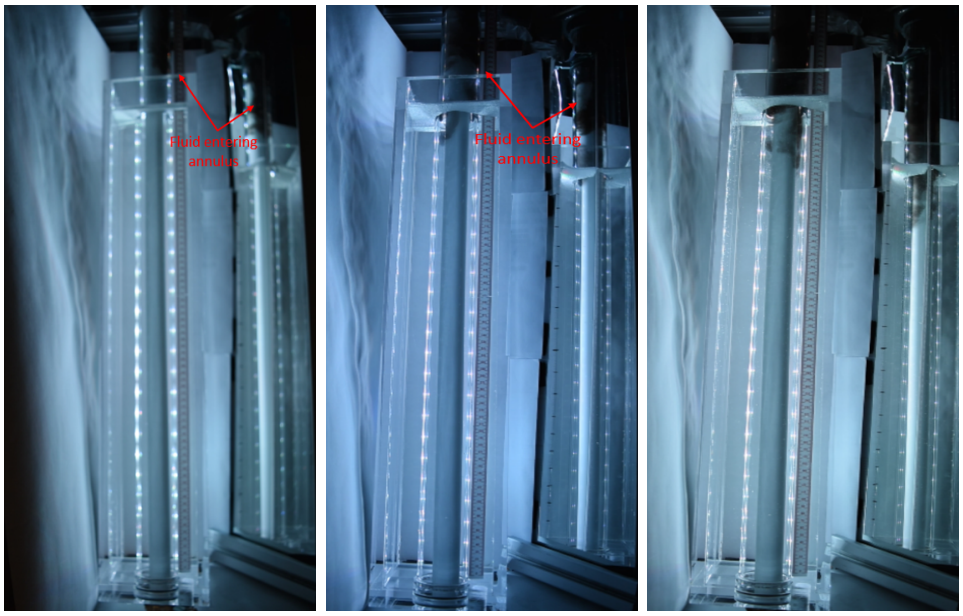

(a) 1.0.1, v=0, At=0,00394 (b) 2.0.1, v=0, At=0,0101 (c) 3.0.2, v=0, At=0,0197

Figure 4.4: Displacement at 10s (no flow)

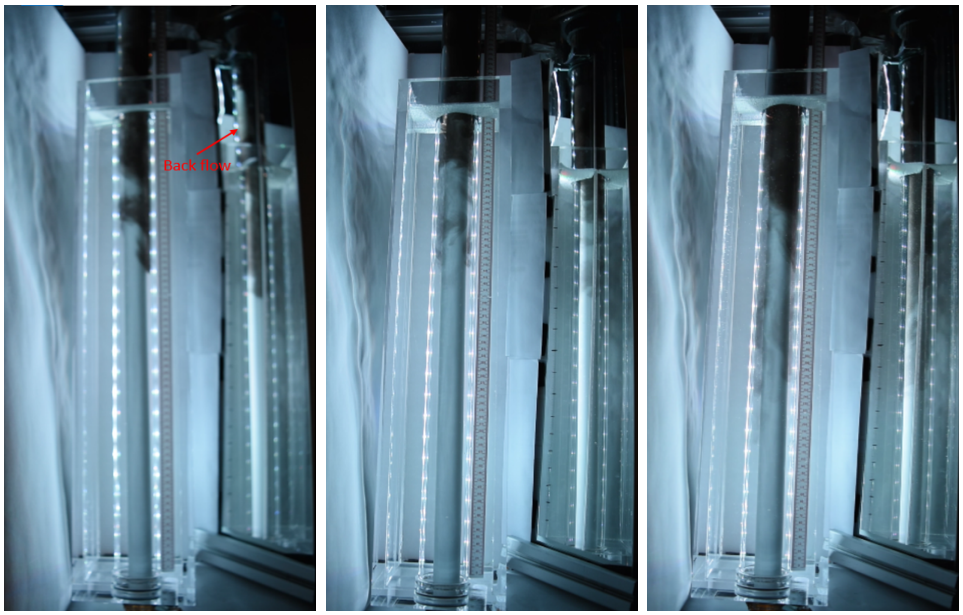

(a) 1.0.1, v=0, At=0,00394 (b) 2.0.1, v=0, At=0,0101 (c) 3.0.2, v=0, At=0,0197

Figure 4.5: Displacement at 30s (no flow)

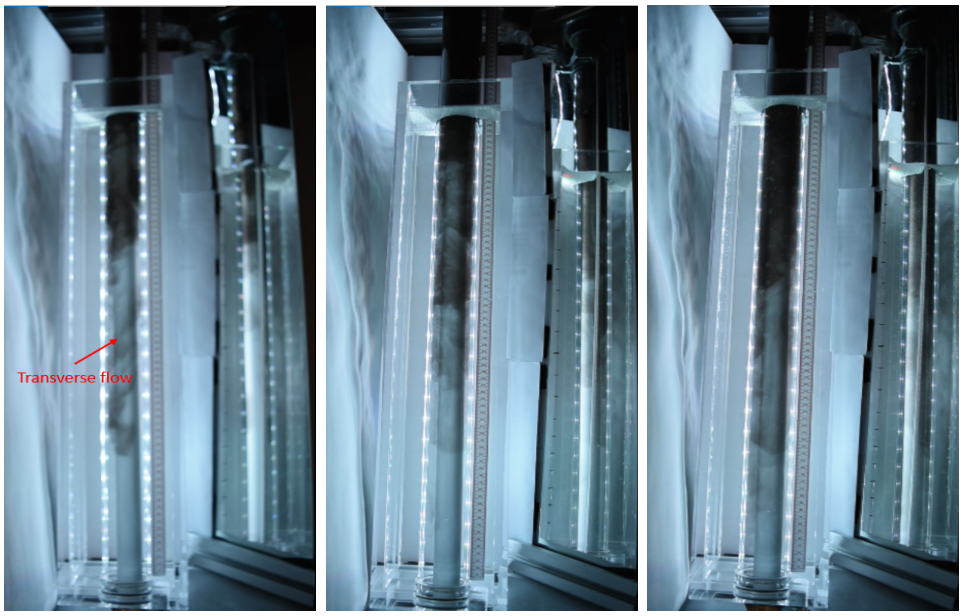

(a) 1.0.1, v=0, At=0,00394 (b) 2.0.1, v=0, At=0,0101 (c) 3.0.2, v=0, At=0,0197

Figure 4.6: Displacement at 60s (no flow)

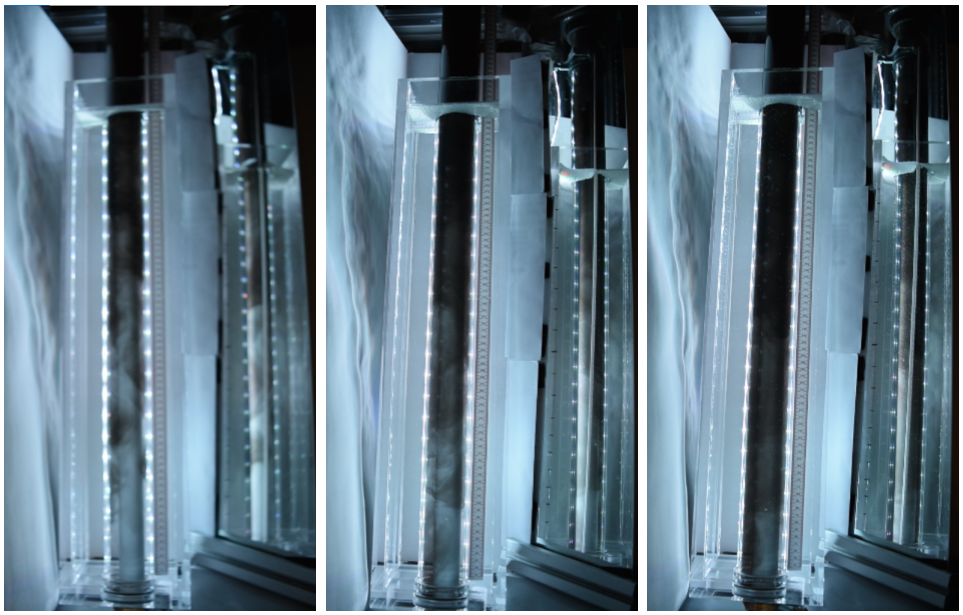

(a) 1.0.1, v=0, At=0,00394 (b) 2.0.1, v=0, At=0,0101 (c) 3.0.2, v=0, At=0,0197

Figure 4.7: Displacement at 120s (no flow)

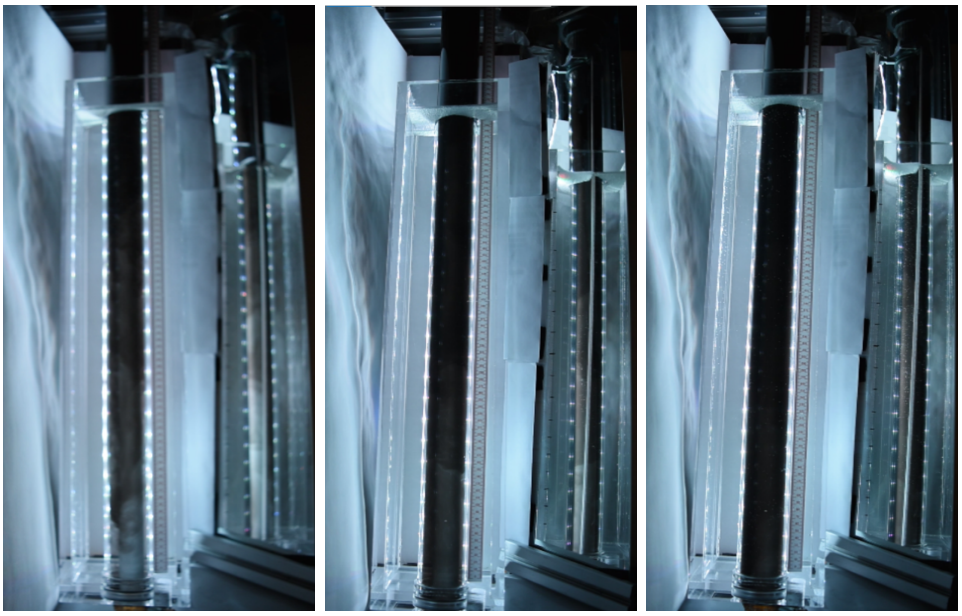

(a) 1.0.1, v=0, At=0,00394 (b) 2.0.1, v=0, At=0,0101 (c) 3.0.2, v=0, At=0,0197

Figure 4.8: Displacement at 240s (no flow)

4.5.2 10 mm/s outlet flow

Figure 4.9-4.12 shows series 1.1.2, 2.1.3 and 3.1.2. When gravity induced flow is introduced the density difference (At) is not as prominent compared to no outlet flow. However, the front still moves at a faster rate with increasing At. The amount of back flow is decreasing as flow is introduced, and transverse flow and downward displacing become more dominant. By looking at the displacements it seems that back flow moves faster upwards with larger At, but it does not move as far up in the annulus as lower At, and is "pushed" back down faster.

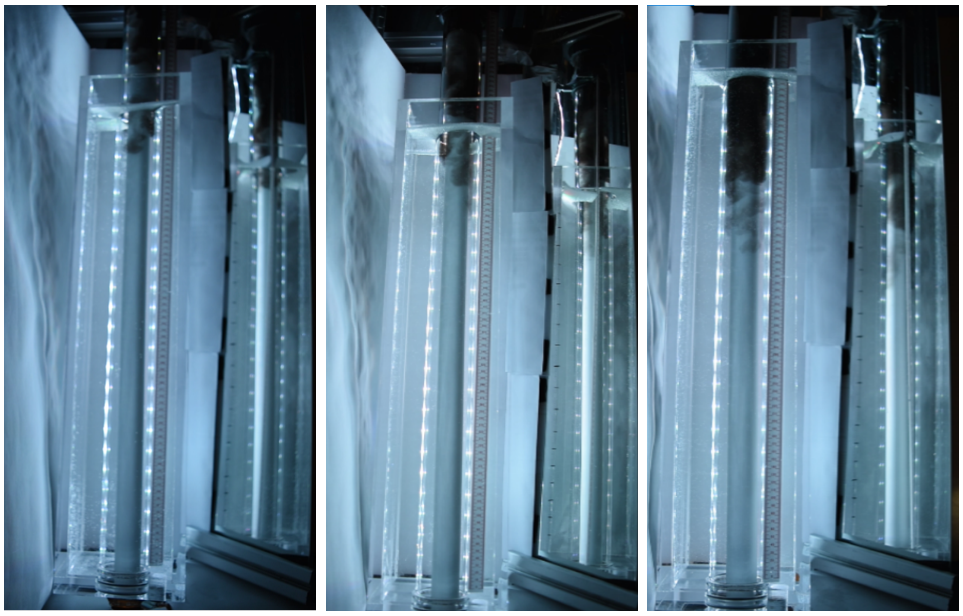

(a) 1.1.2, v=9,44mm/s, At=0,00354 (b) 2.1.3, v=10mm/s, At=0,0103 (c) 3.1.2, v=10,4mm/s, At=0,0198

Figure 4.9: Displacement at 10s (10mm/s)

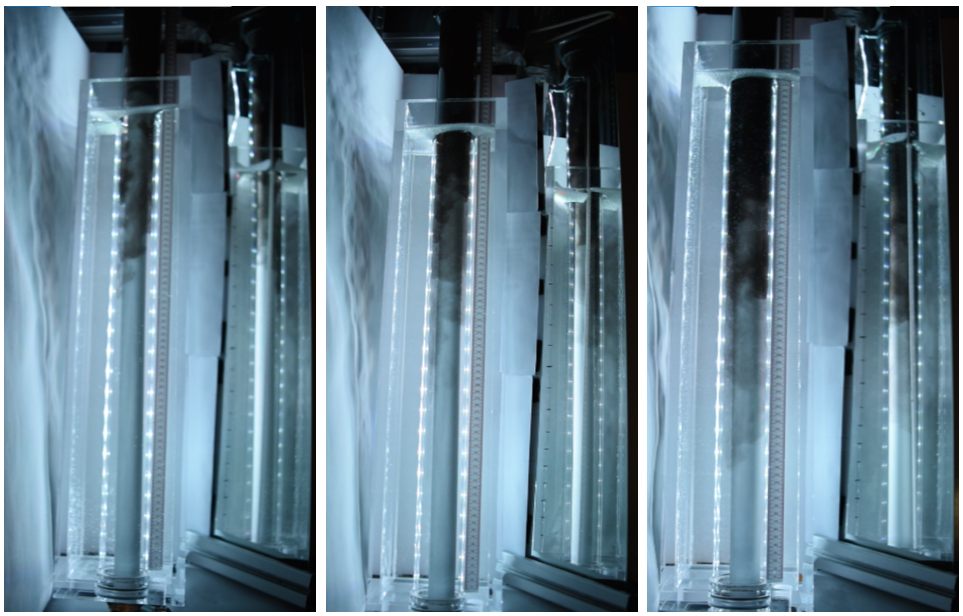

(a) 1.1.2, v=9,44mm/s, At=0,00354 (b) 2.1.3, v=10mm/s, At=0,0103 (c) 3.1.2, v=10,4mm/s, At=0,0198

Figure 4.10: Displacement at 20s (10mm/s)

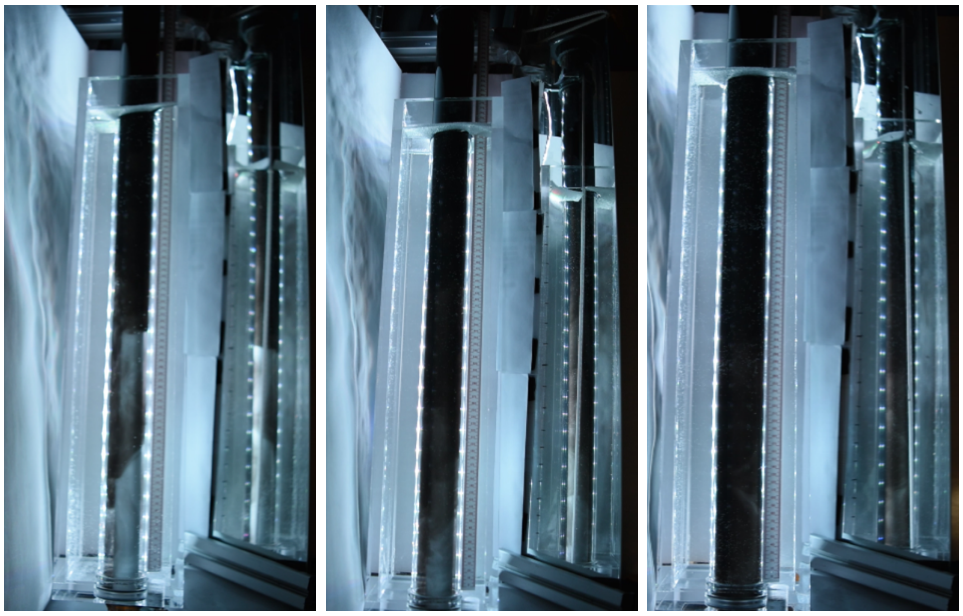

(a) 1.1.2, v=9,44mm/s, At=0,00354 (b) 2.1.3, v=10mm/s, At=0,0103 (c) 3.1.2, v=10,4mm/s, At=0,0198

Figure 4.11: Displacement at 50s (10mm/s)

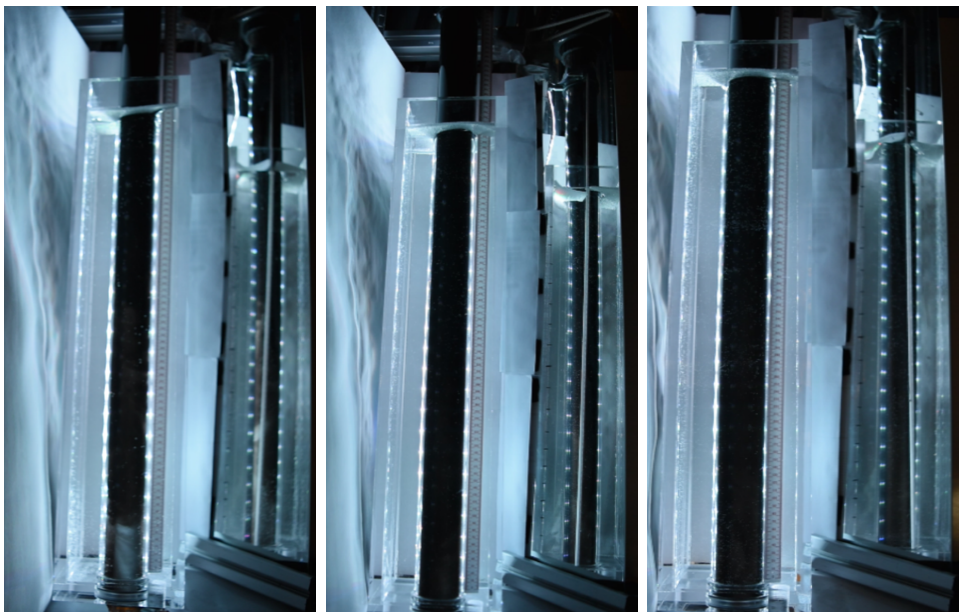

(a) 1.1.2, v=9,44mm/s, At=0,00354 (b) 2.1.3, v=10mm/s, At=0,0103 (c) 3.1.2, v=10,4mm/s, At=0,0198

Figure 4.12: Displacement at 80s (10mm/s)

4.5.3 20mm/s outlet flow

Figure 4.13-4.16 shows the displacement from series 1.2.3, 2.2.3 and 3.2.3. At increasing flow velocities the difference in back flow and transverse flow between the Atwood numbers seems less obvious. This might be because of the increasing speed makes it more difficult to observe, but also the fact that the fluids have less time in the annulus before it is "pushed" out might be a factor giving the fluids less time to mix, this can also be seen in figure 4.3 where increasing velocity leads to a higher volume needed to displace the fluid in the annulus. At higher velocity the flow seems more straight.

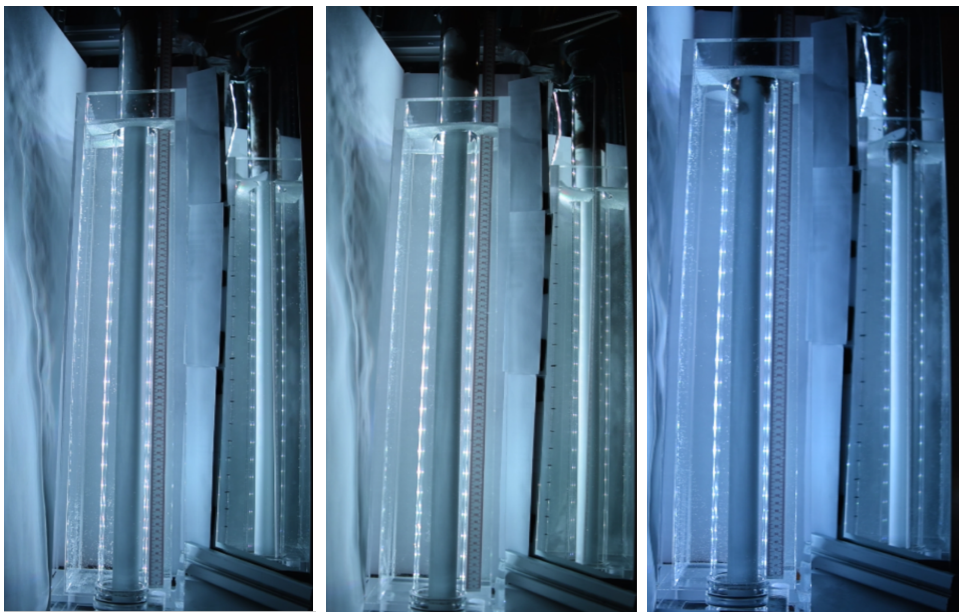

(a) 1.2.3, v=19,5mm/s, At=0,00349 (b) 2.2.3, v=21,9mm/s, At=0,0103 (c) 3.2.3, v=19,6mm/s, At=0,0199

Figure 4.13: Displacement at 3s (20mm/s)

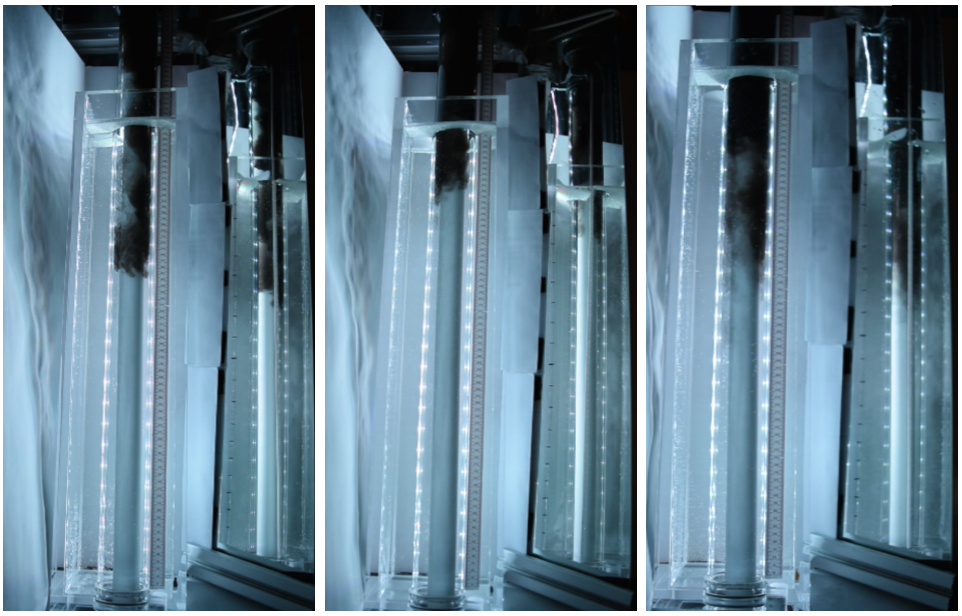

(a) 1.2.3, v=19,5mm/s, At=0,00349 (b) 2.2.3, v=21,9mm/s, At=0,0103 (c) 3.2.3, v=19,6mm/s, At=0,0199

Figure 4.14: Displacement at 10s (20mm/s)

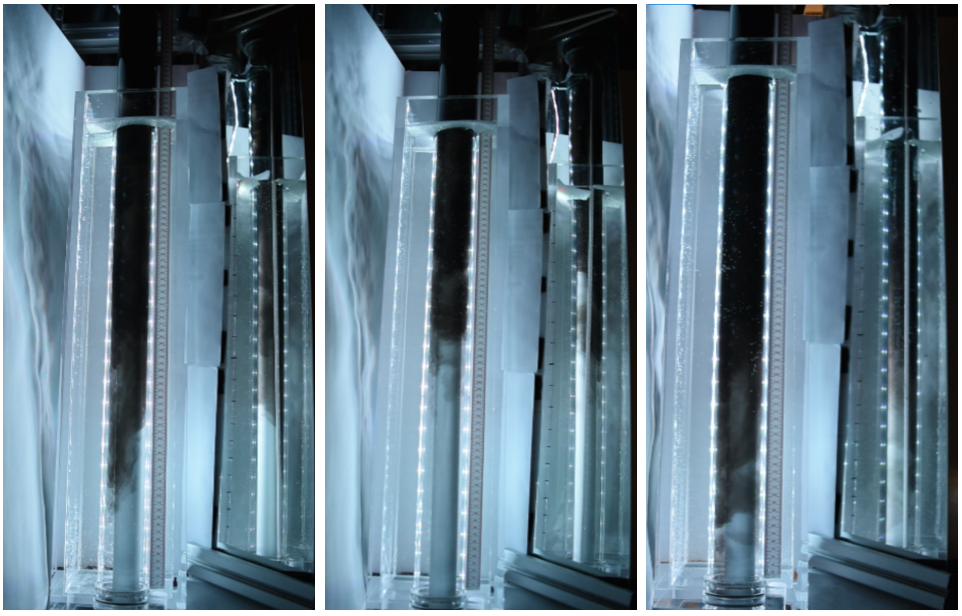

(a) 1.2.3, v=19,5mm/s, At=0,00349 (b) 2.2.3, v=21,9mm/s, At=0,0103 (c) 3.2.3, v=19,6mm/s, At=0,0199

Figure 4.15: Displacement at 20s (20mm/s)

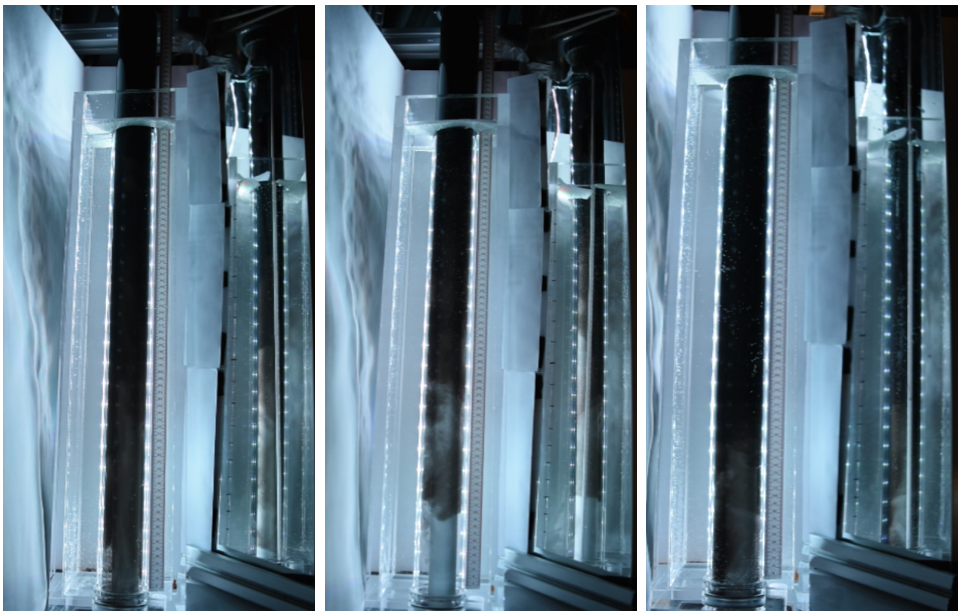

(a) 1.2.3, v=19,5mm/s, At=0,00349 (b) 2.2.3, v=21,9mm/s, At=0,0103 (c) 3.2.3, v=19,6mm/s, At=0,0199

Figure 4.16: Displacement at 30s (20mm/s)

4.5.4 40mm/s outlet flow

Figure 4.17-4.20 shows the displacement of series 1.3.2, 2.3.2 and 3.3.3. Same as for 20mm/s, the downward flow seems to be most dominating in the displacement and the effect of At is not as prominent. However the At does have an effect on displacement time and the volume needed for displacement as seen in 4.2 and 4.3.

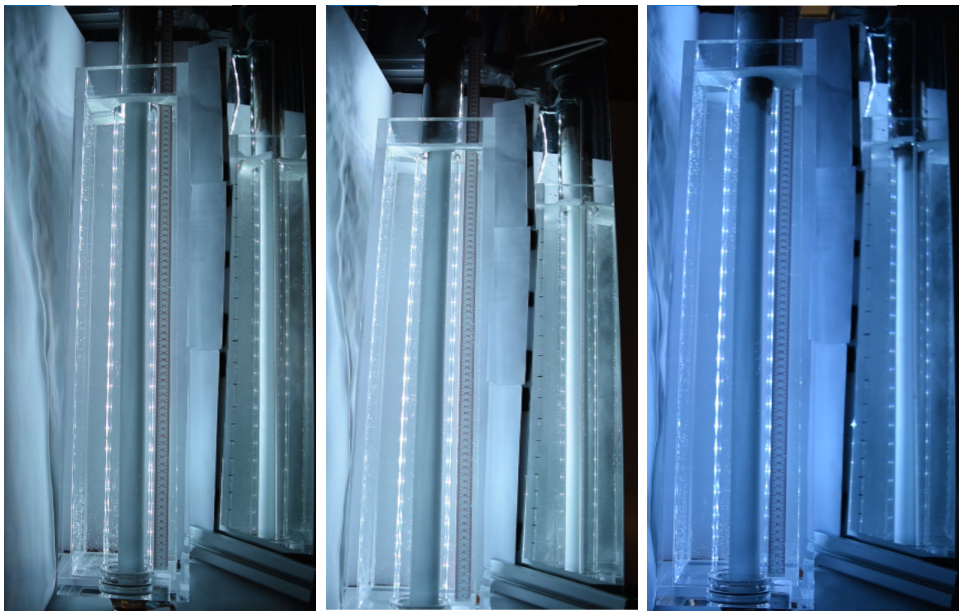

(a) 1.3.2, v=35,5mm/s, At=0,00394 (b) 2.3.2, v=39,8mm/s, At=0,0101 (c) 3.3.3, v=40,5mm/s, At=0,0199

Figure 4.17: Displacement at 2s (40mm/s)

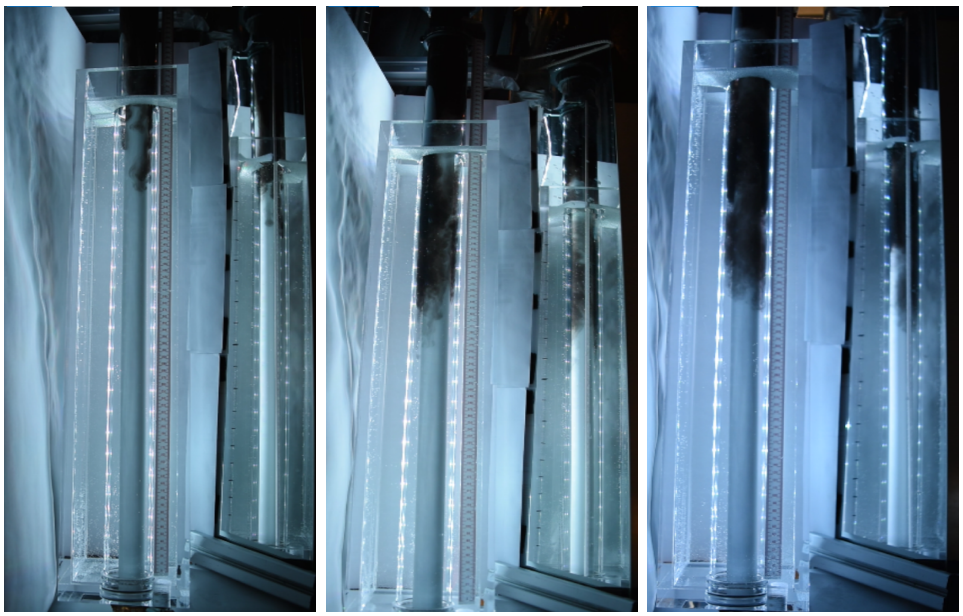

(a) 1.3.2, v=35,5mm/s, At=0,00394 (b) 2.3.2, v=39,8mm/s, At=0,0101 (c) 3.3.3, v=40,5mm/s, At=0,0199

Figure 4.18: Displacement at 5s (40mm/s)

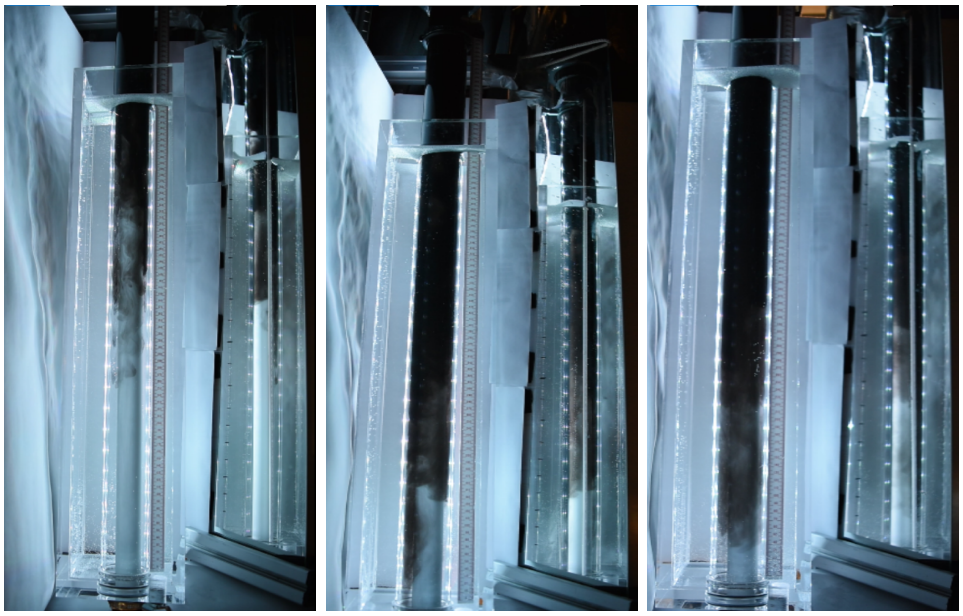

(a) 1.3.2, v=35,5mm/s, At=0,00394 (b) 2.3.2, v=39,8mm/s, At=0,0101 (c) 3.3.3, v=40,5mm/s, At=0,0199

Figure 4.19: Displacement at 10s (40mm/s)

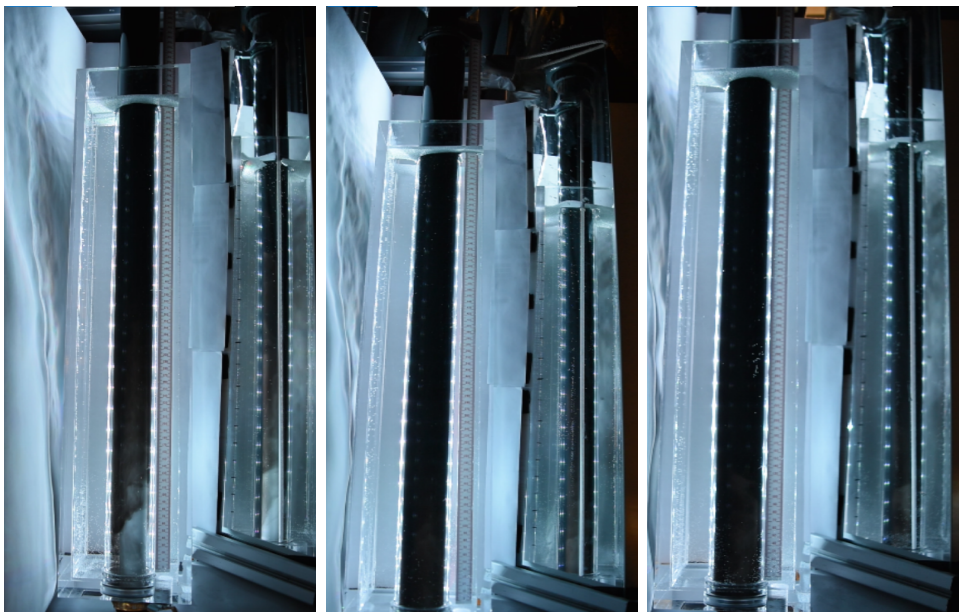

(a) 1.3.2, v=35,5mm/s, At=0,00394 (b) 2.3.2, v=39,8mm/s, At=0,0101 (c) 3.3.3, v=40,5mm/s, At=0,0199

Figure 4.20: Displacement at 20s (40mm/s)

4.6 Effect of flow velocity

The effect of flow velocity was studied by comparing different runs with constant At and varying outlet velocity. It was observed a more violent mixing at the start of the displacing with increasing flow rate. However the mixing seems to settle faster and the heavy fluid "pushes" the back flow downwards to the bottom such that the penetration of light fluid in upwards direction does not reach as far. Overall it seemed that with a higher velocity it was less fingering and a somewhat more even displacement front than for lower velocity.

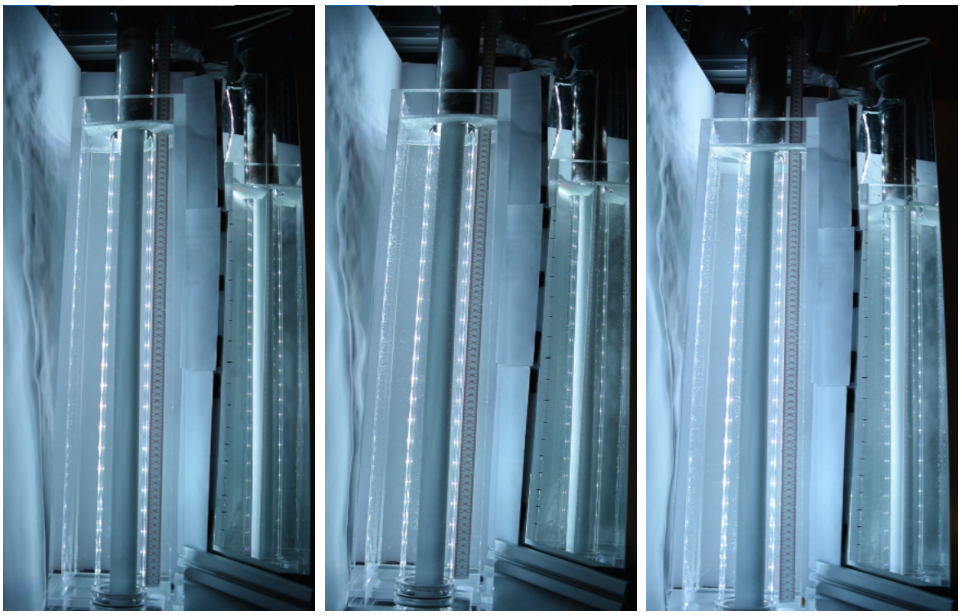

(a) 2.1.1, v=9,29mm/s, t=10s (b) 2.2.1, v=25,3mm/s, t=2s (c) 2.3.1, v=44,1mm/s, t=1s

Figure 4.21: Displacement reached Styrofoam (At=0,0103)

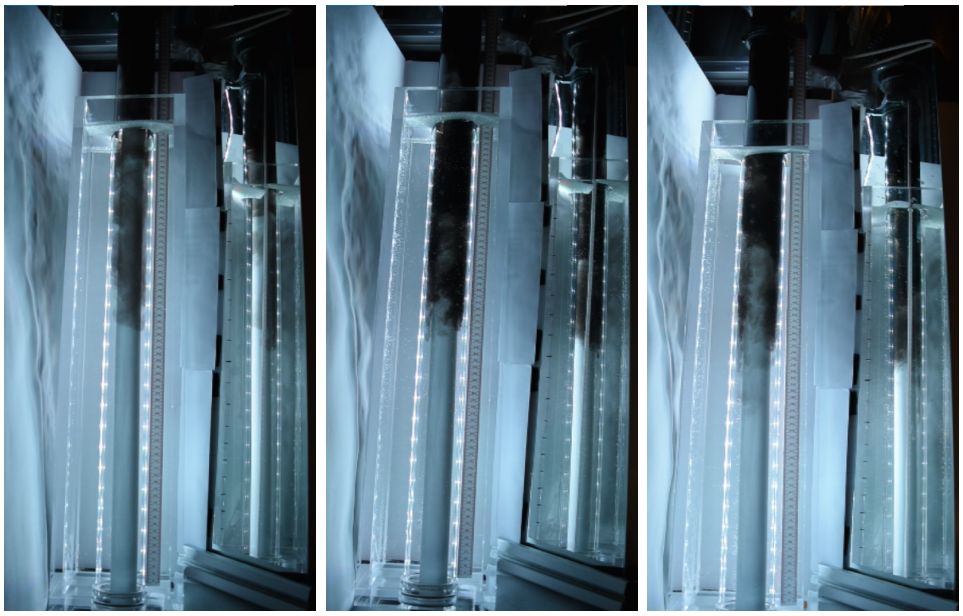

(a) 2.1.1, v=9,29mm/s, t=20s (b) 2.2.1, v=25,3mm/s, t=7s (c) 2.3.1, v=44,1mm/s, t=5s

Figure 4.22: Displacement reached halfway through annulus (At=0,0103)

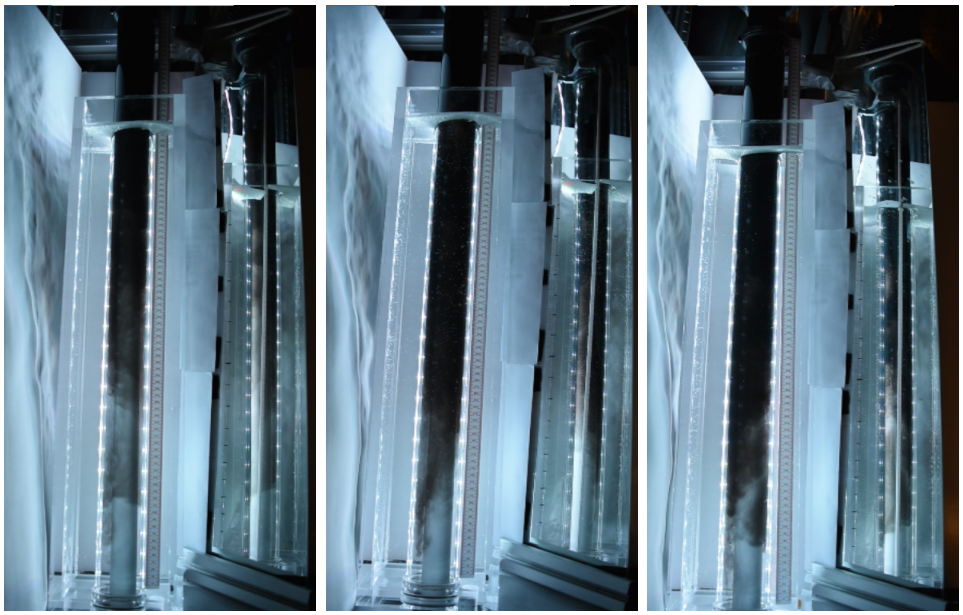

(a) 2.1.1, v=9,29mm/s, t=46s (b) 2.2.1, v=25,3mm/s, t=11s (c) 2.3.1, v=44,1mm/s, t=9s

Figure 4.23: Displacement reached just above bottom (At=0,0103)

4.7 Image analysis

By using the MatLab code provided by Rune W. Time (see appendix C.2) the front can be analysed by studying the brightness of the image pixels. The black heavy fluid has a low red, green and blue intensity while the opposite is true for the transparent light fluid letting the LED-light through. Figure 4.24 shows analysis of the image of displacement 6.12s after the ball valve is opened for run 3.3.3, and this is the reference picture. The image at the top is of the annulus and the x axis is pixels in the vertical (downward) direction, while the y axis in horizontal direction. The red line in the image shows the middle of the area analysed, and the area is 40 pixels wide on each side of the red line making up 81 pixel cross-section in total for the horizontal direction. The blue line in the first graph represent the brightness along the red middle line in the top picture. The red line in the bottom graph is an averaged pixel brightness along the cross-section of the annulus. The length scale on the image is 24 pixels/cm. The next two figures (4.25 and 4.26) is the same displacement after 1s and 2s from the reference. The black slope in the graphs represent the front of the reference image. As seen in the picture there are some trapped light fluid from x=800 in the first figure till in the last x=950. This is what makes the small spike behind the front in the graphs. The front moves from approximately x=1200 in the reference (4.24) to x=1500 last figure (4.26). This is a movement of about 125mm over 2s giving a front velocity of approximately 62.5mm/s.

4.7 Image analysis

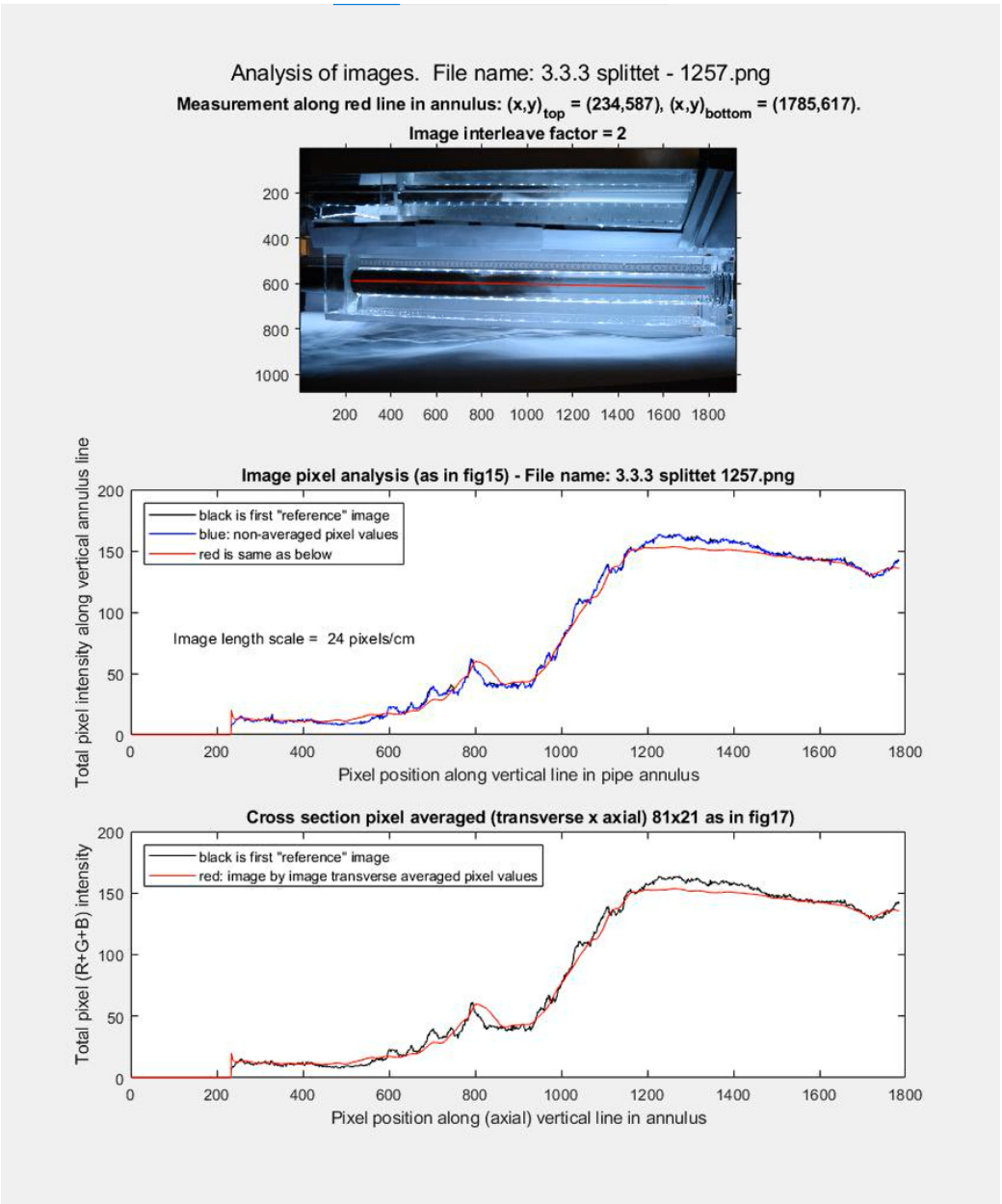

Figure 4.24: Image analysis at t=6.12s

4.7 Image analysis

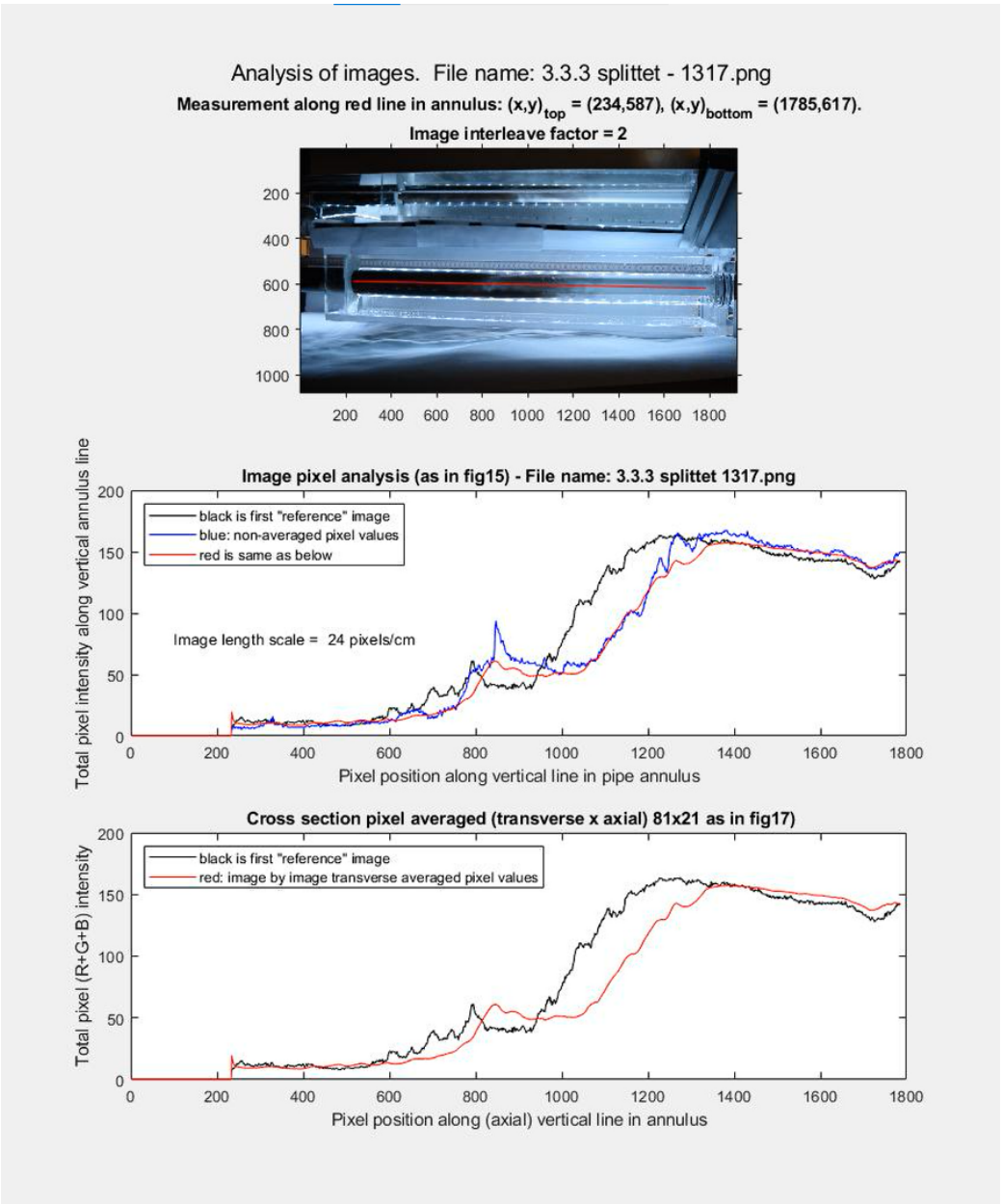

Figure 4.25: Image analysis at t=7.12s

4.7 Image analysis

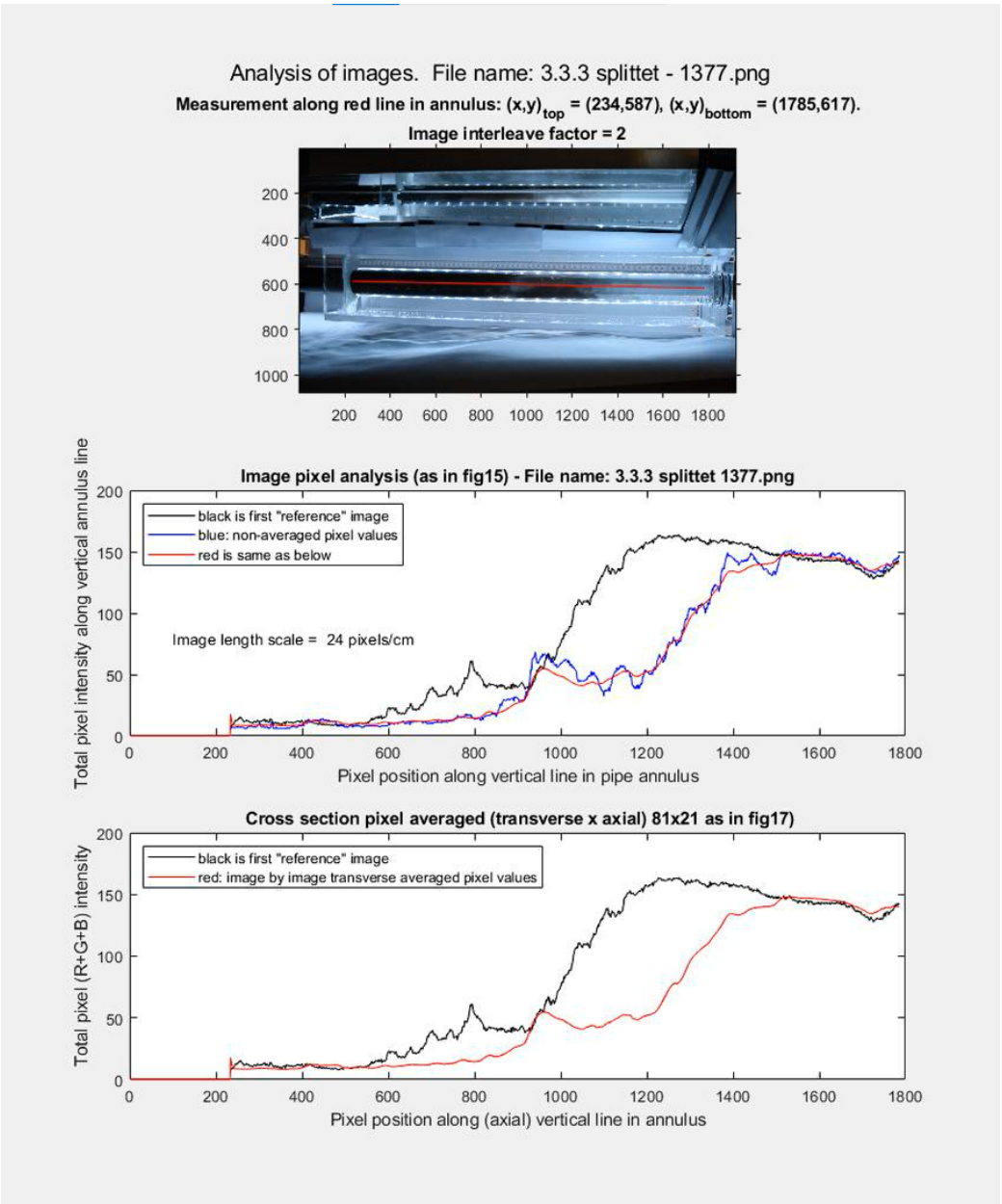

Figure 4.26: Image analysis at t=8.12s

Chapter 5

Conclusion

Mixing, transverse flow and back flow was observed in all the experiments conducted. The transverse flow spreads the front around the annulus and back flow gives a counter-current flow of light fluid leading to a diffusive mixing. The concentration of black ink in the front of the flow is observed to be less due to mixing.

At no outlet flow and 10mm/s flow the density difference (At) is seen to play a larger role in displacement of the light fluid. The runs without outlet flow the density difference is what drives the exchange flow. With increasing At the displacement is observed to moves at a larger rate and the back flow of light fluid does not penetrate as far into the heavy fluid as for lower At.

As flow velocity increases the effect of density difference decreases and the flow becomes the dominating factor for displacement. Flow of light fluid in counter-current direction seems to be interrupted by the downward flow and "pushed" back down.

The MatLab code provided by Rune W. Time is shown where the front velocity and the back flow can be studied. Unfortunately there was only time to look at one of the displacements and further study of this is recommended in the next section.

5.1 Recommendation for further work

In this study miscible fluids with constant viscosity was used. Introducing for instance glucose to the fluid to alter the viscosity would be interesting such that the effect of viscosity could be studied. Also looking at immiscible fluids would be an idea.

Furthermore, the annulus is not always vertical in the field so studying the displacement in horizontal or inclined setups to see the difference when gravity is working in a different direction compared to the flow.

It was discovered after the experiments was done that the inner pipe in the setup was not a 100% concentric, to get a better understanding of displacement in a concentric annulus the inner pipe should be looked at and adjusted. Moreover, a setup where the inner pipe could be moved to see the effects of eccentricity on the displacement could also be considered.

5.1 Recommendation for further work

Although the initial plan was to look at the front velocity with the MatLab script, this was not completed. Improving this script to apply for all the experimental runs to compare front velocities and also detect amount of back flow would improve the results.

Improvements to the experimental setup:

The fish tank used in the experiment is placed around 30cm below the ball valve separating the heavy and light fluid. This makes it more difficult to study the initial displacement after the ball valve is opened. Moving the fish tank further up such that it is closer to the ball valve should be considered. Another improvement that could be made is to find a better place for the camera stand to be mounted. The camera is mounted to the same ladder that is used to open the ball valve. This makes the first few seconds a bit shaky for the camera as the person who opens the ball valve has to climb down the ladder after it is opened.

References

[1] E. Kuru and S. Seatter, "Reverse Circulation Placement Technique vs. Conventional Placement Technique: A Comparative Study of Cement Job Hydraulics Design," *Journal of Canadian Petroleum Technology*, vol. 44, no. 07, pp. 16–19, Jul. 2005. DOI: 10.2118/05-07-TN1.

[2] S. PELIPENKO and I. FRIGAARD, "Mud removal and cement placement during primary cementing of an oil well part 2; steady-state displacements," *Journal of Engineering Mathematics*, vol. 48, pp. 1–26, 2004.

[3] Schlumberger, *Primary cementing*. [Online]. Available: https://www.glossary.oilfield.slb.com/en/Terms/p/primary_cementing.aspx, (accessed: 10.05.2021).

[4] E. B. Nelson and D. Guillot, *Well Cementing*, 2nd ed. Sugar Land, Texas: Schlumberger, 2006.

[5] D. K. Smith, *Cementing*, 2nd ed. New York City: Henry L. Doherty Memorial Fund of AIME, SPE, 1990.

[6] *High-Temperature Wells with Lost-Circulation Demands and Reverse Circulation Placement Technique Using Foamed Cement Systems: Two Case Histories*, vol. All Days, Paper presented at the SPE Annual Technical Conference and Exhibition, Denver, Colorado, Oct. 2003. DOI: 10.2118/84563-MS.

[7] *Reverse Circulation of Cement on Primary Jobs Increases Cement Column Height Across Weak Formations*, vol. All Days, SPE Oklahoma City Oil and Gas Symposium / Production and Operations Symposium, SPE-25440-MS, Mar. 1993. DOI: 10.2118/25440-MS. eprint: https://onepetro.org/SPEOKOG/proceedings-pdf/93POS/All-93POS/SPE-25440-MS/1981767/spe-25440-ms.pdf. [Online]. Available: https://doi.org/10.2118/25440-MS.

[8] Princton University, *What is viscosity?* [Online]. Available: https://www.princeton.edu/~gasdyn/Research/T-C_Research_Folder/Viscosity_def.html, (accessed: 26.04.2021).

[9] S. PELIPENKO and I. FRIGAARD, "Visco-plastic fluid displacements in near-vertical narrow eccentric annuli: Prediction of travelling-wave solutions and interfacial instability," *Journal of Fluid Mechanics*, vol. 520, pp. 343–377, 2004. DOI: https://doi.org/10.1017/S0022112004001752.

[10] G. I. Barenblatt, "Dimensional analysis and physical similarity," in *Scaling*, ser. Cambridge Texts in Applied Mathematics. Cambridge University Press, 2003, pp. 12–51. DOI: 10.1017/CBO9780511814921.004.

[11] T. Benson, *Reynolds number*. [Online]. Available: https://www.grc.nasa.gov/WWW/BGH/reynolds.html, (accessed: 26.04.2021).

[12] EngineeringLibrary, *Laminar and turbulent flow*. [Online]. Available: https://engineeringlibrary.org/reference/laminar-and-turbulent-fluid-flow-doe-handbook, (accessed: 15.05.2021).

[13] J. Matsumoto, M. A. Aloy, and M. Perucho, "Linear theory of the Rayleigh–Taylor instability at a discontinuous surface of a relativistic flow," *Monthly Notices of the Royal Astronomical Society*, vol. 472, no. 2, pp. 1421–1431, Aug. 2017. DOI: 10.1093/mnras/stx2012.

[14] P. RAMAPRABHU and M. J. ANDREWS, "Experimental investigation of rayleigh–taylor mixing at small atwood numbers," *Journal of Fluid Mechanics*, vol. 502, pp. 233–271, 2004. DOI: 10.1017/S0022112003007419.

[15] D. Sharp, "An overview of rayleigh-taylor instability," *Physica D: Nonlinear Phenomena*, vol. 12, no. 1, pp. 3–18, 1984. DOI: https://doi.org/10.1016/0167-2789(84)90510-4.

[16] D. L. Youngs, "Three-dimensional numerical simulation of turbulent mixing by rayleigh–taylor instability," *Physics of Fluids A: Fluid Dynamics*, vol. 3, pp. 1312–1320, 1991. DOI: https://doi.org/10.1063/1.858059.

[17] L. Gramer, "Kelvin-helmholtz instabilities," May 2007. [Online]. Available: https://www.researchgate.net/publication/228394911_Kelvin-Helmholtz_Instabilities.

[18] D. K. Israel, *14 gorgeous kelv-helmz cloud formations*. [Online]. Available: https://www.mentalfloss.com/article/29587/14-gorgeous-kelv-helmz-cloud-formations, (accessed: 04.06.2021).

[19] F. M. White, *VISCOUS FLUID FLOW*, 2nd. New York: McGraw-Hill Inc., 1991.

[20] J. Pedlosky, *Geophysical Fluid Dynamics*, 2nd. New York: Springer-Verlag, 1987.

[21] COMSOL, *Navier-stokes equation*. [Online]. Available: https://www.comsol.com/multiphysics/navier-stokes-equations?parent=modeling-conservation-mass-energy-momentum-0402-432-302, (accessed: 01.06.2021).

[22] H. J. Skadsem, personal communication, May, 2021.

[23] C. Bjørnsen, "An experimental investigation of density-unstable displacement in a vertical annulus with relevance to "reverse heavy over light" cementing technology," M.S. thesis, Department of petroleum Engineering, Stavanger, 2020.

[24] Endress+Hauser, *The electromagnetic flow measuring principle*, YouTube, Jul. 2009. [Online]. Available: `https://www.youtube.com/watch?v=f949gpKdCI4&ab_channel=Endress%5C%2BHauser`, (accessed: 06.05.2021).

[25] Anton Paar, Ed., *Instruction manual dma 4100 m dma 4500 m dma 5000 m*, 2.21 ed., Austria: Anton Paar GmbH, 2012.

[26] V. K. Singh, *Extracting & saving frames from a video file using matlab code*, 2013. [Online]. Available: `http://www.divilabs.com/2013/11/extracting-saving-of-frames-from-video.html#ixzz3nuCp9nS4`, (accessed: 01.03.2021).

[27] R. W. Time, *Example_script_imageanalysis_folder333splittet_extended_v1*, 2021.

Appendix A

Calibration

A.1 Flow meter

The flow meter was calibrated by filling up the rig with water and measure the flow rate manually at different outlet valve openings. The flow rate was measured by filling up a 5000ml container and timing it with a stopwatch. This was done two times, with roughly the same degree of opening, at four different valve openings. Table A.1 shows the different voltages and the time it took to fill 5000ml of water.

Table A.1: Calibration of flow meter

Test	**Volt**	**Opening (degrees)**	**Time(s)**	**Flow (ml/s)**
1	1,2100	25,00	558,00	8,96
2	1,3788	30,00	246,00	20,30
3	1,6597	35,00	121,00	41,32
4	1,9875	40,00	79,00	63,29
5	2,1644	40,00	66,00	75,75
6	1,7840	35,00	102,00	49,00
7	1,3680	30,00	253,00	19,76
8	1,1860	25,00	666,00	7,51

After the measurements was done the flow rate vs voltage was plotted in Excel (see figure A.1) and a best fit line was found from the plot resulting in the equation:

$$y = 70.055x - 75,812 \tag{A.1}$$

where y is the flow rate and x is the volt.

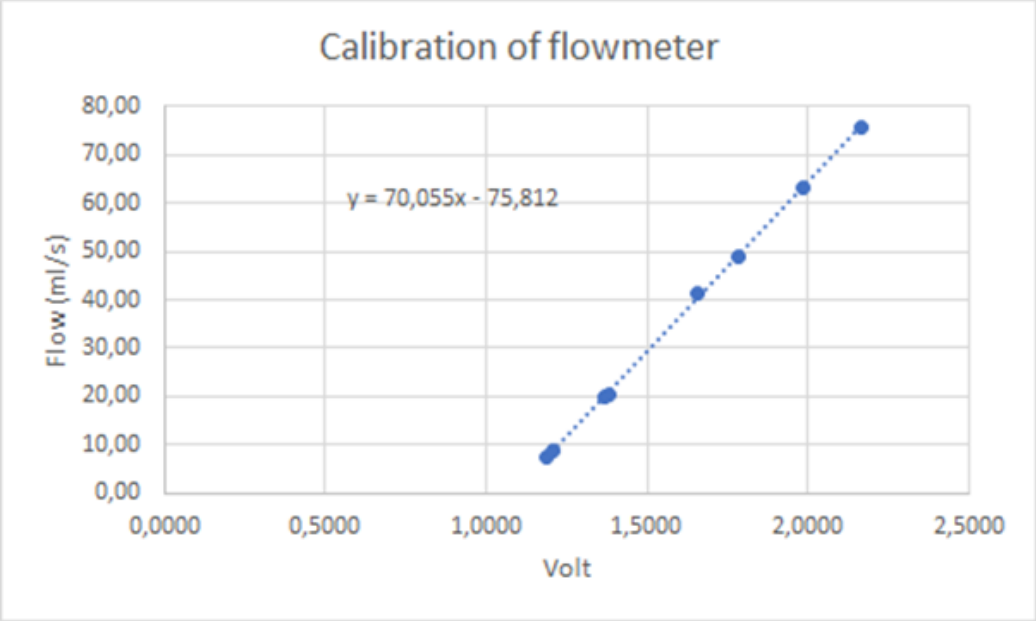

Figure A.1: Best fit line for Flow rate vs. Volt

A.2 Pressure sensor

The pressure sensor was calibrated by previous master student C. Bjørnsen. This was done by filling up the cylinder with water and measuring the height of water above the pressure sensor. Further, the theoretical hydraulic pressure was calculating using:

$$P = \rho g h \tag{A.2}$$

and compared to the Pasco pressure data. The measured data and theoretical values differs about 30 mbar which indicates good measurements. The pressure test was done three times shown in figure A.2, A.3 and A.4, and then plotted against theoretical pressure in Excel as seen in figure A.5 [23].

A.2 Pressure sensor

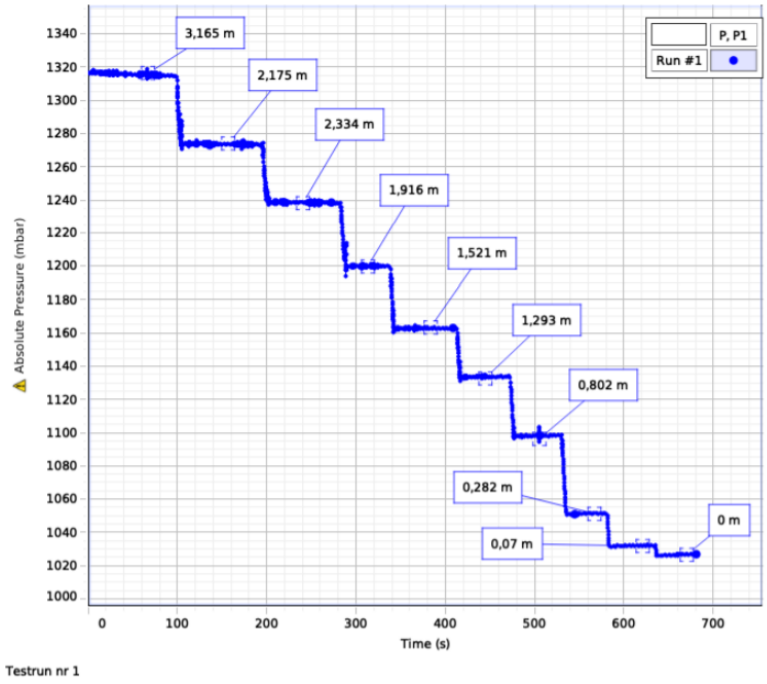

Figure A.2: 1st test run for pressure calibration [23]

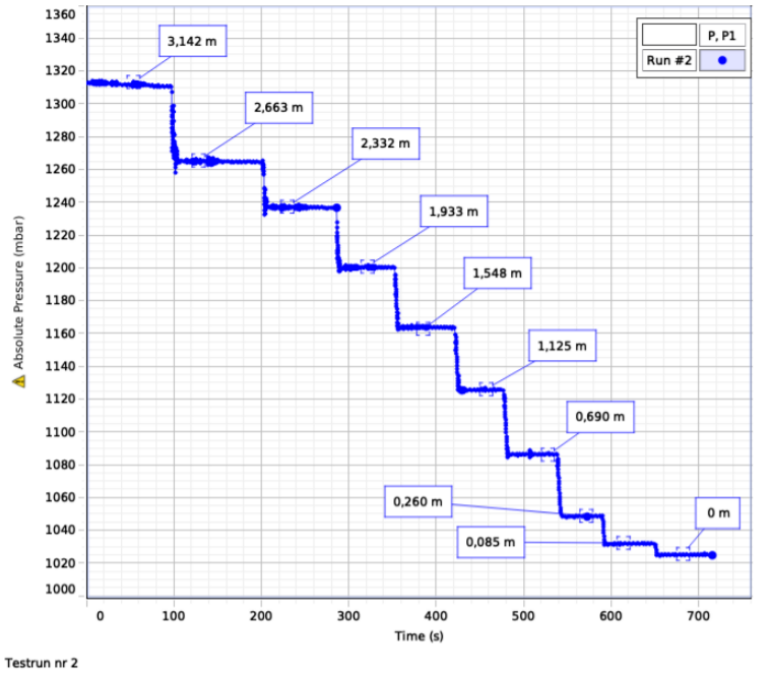

Figure A.3: 2nd test run for pressure calibration [23]

A.2 Pressure sensor

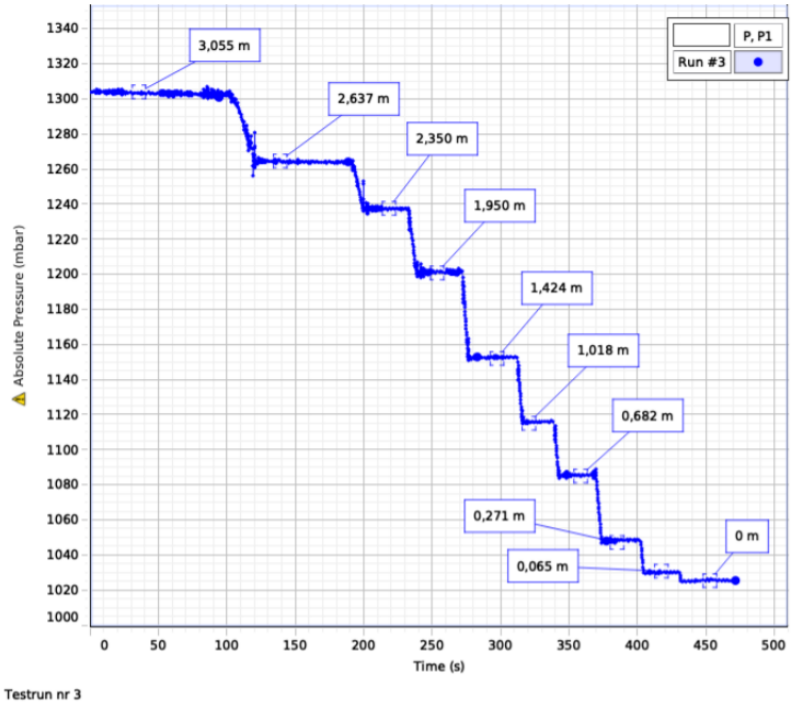

Figure A.4: 3rd test run for pressure calibration [23]

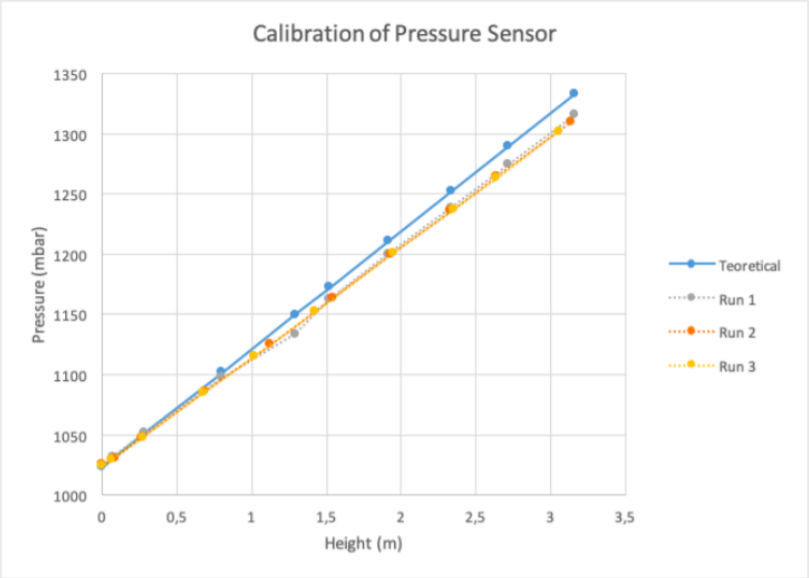

Figure A.5: Theoretical pressure and the three pressure tests plotted in Excel [23]

Appendix B

Heavy fluid

Table B.1: Specification of heavy fluid for each run

Series	**Solution (per 100ml distilled water)**	**Density (g/cm^3)**	**Temperature (°C)**	**At**
1.0.1-1.0.3	1g salt(NaCl)	1,0051	20,03	0,00394
1.1.1-1.1.2	1g salt(NaCl)	1,0054	20,03	0,00354
1.1.3	1g salt(NaCl)	1,0054	20,04	0,00354
1.2.1-1.2.3	1g salt(NaCl)	1,0053	20,03	0,00349
1.3.1-1.3.2	1g salt(NaCl)	1,0053	20,02	0,00349
1.3.3	1g salt(NaCl)	1,0054	20,05	0,00354
2.0.1-2.0.3	3g salt(NaCl)	1,0188	20,02	0,0101
2.1.1	3g salt(NaCl)	1,0191	19,99	0,0103
2.1.2-2.3.2	3g salt(NaCl)	1,0191	20,02	0,0103
2.3.3	3g salt(NaCl)	1,0191	20,05	0,0103
3.0.1-3.0.3	3g salt(NaCl)	1,0385	20,02	0,0197
3.1.1-3.1.3	6g salt(NaCl)	1,0387	20,02	0,0198
3.2.1-3.2.3	6g salt(NaCl)	1,0389	20,01	0,0199
3.3.1-3.3.3	6g salt(NaCl)	1,0389	20,02	0,0199

B.1 Visibility test

1 ml ink was used per 1000ml of distilled water.

Figure B.1: Heavy fluid with lissamine as colorant

Figure B.2: Ink used

B.1 Visibility test

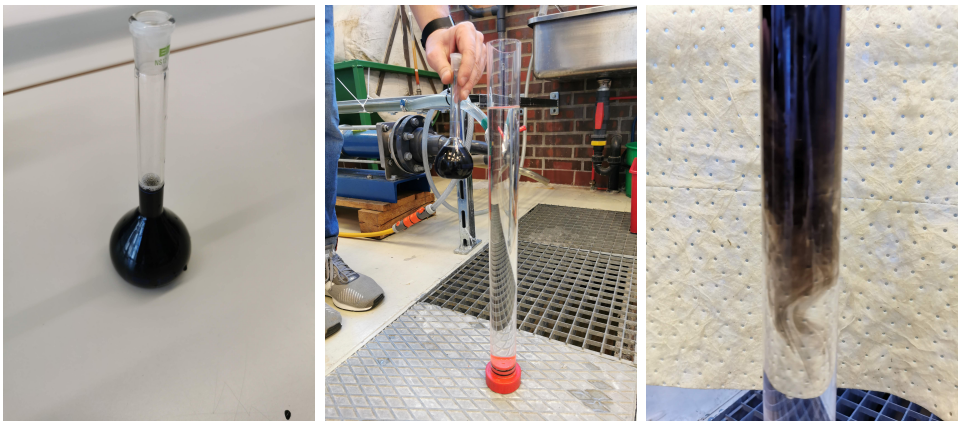

Figure B.3: Visibility of ink in a glass tube

Appendix C

MatLab scripts

C.1 Video split

```
1
2  %%Extracting & Saving of frames from a Video file through ...
       Matlab Code%%
3  clc;
4  close all;
5  clear all;
6  % Tested 8.10.2015 by Benja
7
8  % assigning the name of sample avi file to a variable
9  filename = 'test 1.0.3 0flow.MOV';
10
11 %reading a video file
12 mov = VideoReader(filename);
13
14 % Defining Output folder as 'snaps'
15 opFolder = fullfile(cd, '1.0.3 splittet');
16 %if  not existing
17 if ¬exist(opFolder, 'dir')
18 %make directory & execute as indicated in opfolder variable
19 mkdir(opFolder);
20 end
21
22 %getting no of frames
23 numFrames = mov.NumberOfFrames;
24
25 %setting current status of number of frames written to zero
26 numFramesWritten = 0;
27
28 %for loop to traverse & process from frame '1' to 'last' ...
       frames
29 for t = 1 : numFrames
30 currFrame = read(mov, t);    %reading individual frames
31 opBaseFileName = sprintf('%3.3d.png', t);
32 opFullFileName = fullfile(opFolder, opBaseFileName);
33 imwrite(currFrame, opFullFileName, 'png');   %saving as ...
       'png' file
34 %indicating the current progress of the file/frame written
```

```
progIndication = sprintf('Wrote frame %4d of %d.', t, ...
    numFrames);
disp(progIndication);
numFramesWritten = numFramesWritten + 1;
end      %end of 'for' loop
progIndication = sprintf('Wrote %d frames to folder ...
    "%s"',numFramesWritten, opFolder);
disp(progIndication);
%End of the code

% Read more:
%http://www.divilabs.com/2013/11/extracting-saving-of- ...
%frames-from-video.html#ixzz3nuCp9nS4
```

[26]

C.2 Front analysis

```
% Script to read and plot images from folder "3.3.3 splittet"

clear all
clf
clc
format compact

% For pixel averaging purposes
Nf = 40 % Gives rectangle 2*Nf+1 pixels wide (WIDTH)
Mf = 5  % Gives 2*Mf+1 pixels long (AXIAL LENGTH)

% This folder name you need to adapt to your own computer:
mappenavn= 'C:\Master og bachelor 2021 - pÃ¥ C ...
    hjemme\3.3.3 splittet - fra 1249 - pÃ¥ pc hjemme\'
files = dir(mappenavn) %Leser inn filoversikt i mappen

% Make a list of files in your folder, e.g. like here:
for i= 1:20  % Skriv ut en liste, feks av de fÃ¸rste 20 filene
    % for Ã¥ se at alt er som det skal
    files(i+8).name
end

% FÃ˜RST: Les inn og beregn et bilde som kan vÃ¦re farge ...
    og posisjons
% referanse for bilder etterpÃ¥
navn1 = [mappenavn files(10).name] % Picks out just file ...
    number 10 in the list
bilde1 = navn1 % Original bilde - navn
```

```
26
27 % Read original images into "bilete"
28 [bilete, mappe] = imread(bilde1); % Only 8 bit = 255 ...
       intensity values in "bilete"
29
30 % Now convert from uint8 to double precision with higher ...
       pixel intensity resolution
31 DDbilete1 = double(bilete);  %DDbilete1 = Originalbilde ...
       konvertert til double
32
33 figure(1)
34 subplot(2,1,1)
35 imshow(bilde1) ; % Just to show the original image (uint8 ...
       format)
36
37 subplot(2,1,2)
38 imshow(bilete) ; % Double precision format
39 hold on
40 % Coordinates for a given analysis line
41 annxtop = 234; annxbot = 1785;
42 annytop = 587; annybot = 617;
43 annxline = [annxtop annxbot];
44 annyline = [annytop annybot];
45 DXann = annxbot-annxtop
46 DYann = annybot-annytop
47
48 title(['Measurement along red line in annulus: (x,y)_{top} ...
       = ('...
49     num2str(annxtop) ',' num2str(annytop) '), ...
           (x,y)_{bottom} = (' ...
50     num2str(annxbot) ',' num2str(annybot) ').'])
51
52 axis('image')
53 plot(annxline,annyline,'-r')
54 xlabel('x pixel position')
55 ylabel('y pixel position')
56 nn=10
57 FIL = ['File name: 3.3.3 splittet - ' files(nn).name]
58 sgtitle(['Analysis of images.  ' FIL])
59 hold off
60
61 % ***************** EXTENDED VERSION - to analyse series of ...
       images ********
62 % **** MAKE A FIRST REFERNCE IMAGE - for comparison as ...
       time evolves ******
63 % ********************************************************
64 originalbilde = 'no pixel averaging'
65 % ********************************************************
66
```

```
67 % *********** LENGTH SCALE ("manually") from bilde ... 1381.png: **********
68 nullen = 1799 % <--x og y = 542
69 tretti = 1080 % <--x og y = 530
70 % Antall pixler per millimeter:
71 xlengdeskala = (nullen-tretti)/30
72
73 % ************************************    FIGUR3  ... ************************
74 figure(3) % Plott farge variasjonen langs en nesten ... vertikal linje i
75 % annulus original bilde uten midling av nabopunkter
76 % ************************************************
77
78 for ix=annxtop:annxbot
79     %ylin = annytop + round(DYann*(ix-annytop)/DXann);     ... % MÃ¥ ha vÃ¦rt feil!!
80     ylin = annytop + round(DYann*(ix-annxtop)/DXann); % ... Endelig riktig!
81     fargeannR(ix)= DDbilete1(ylin,ix,1); % Double precision
82     fargeannG(ix)= DDbilete1(ylin,ix,2);
83     fargeannB(ix)= DDbilete1(ylin,ix,3);
84 end
85 fargediff=abs(fargeannB-fargeannR);
86 fargesum =(fargeannR+fargeannG+fargeannB)/3;
87 Difflager1=fargesum; % fargeannB %fargediff;
88 hold on
89 subplot(4,1,1)
90 plot(fargediff,'k')
91 % plot(fargesum,'k')
92 %        title ('Light intensities along line in annulus - ... no averaging')
93 title(['Measurement along red line in annulus: (x,y)_{top} ... = ('...
94     num2str(annxtop) ',' num2str(annytop) '), ... (x,y)_{bottom} = (' ...
95     num2str(annxbot) ',' num2str(annybot) ')' ])
96 legend('Red minus green - compensates for light variations')
97 subplot(4,1,2)
98 plot(fargeannR,'r')
99 legend('Red only')
100 subplot(4,1,3)
101 plot(fargeannG,'g')
102 legend('Green only')
103 ylabel('Pixel intensity (red color plane)')
104 subplot(4,1,4)
105 plot(fargeannB,'b')
106 legend('Blue only')
107 xlabel('Pixel position in image')
```

```
108 hold off
109
110 % ************ NOW START LOOP OVER IMAGES ...
      ********************************
111 nnstart=10
112 nnstop=nnstart+120
113 Hoppover = 2 % Image interleave factor
114
115 for nn = nnstart:Hoppover:nnstop
116     % pause(1)
117     filnavn = files(nn).name
118     navn2 = [mappenavn filnavn] %
119     J = nn+1 %indekser fra 1 og oppover pga nn=0
120
121     iles=1
122     if iles==1 % Lese sekvens av nye bilder etter ...
            referanse bildet
123         bilde2 = navn2
124         [bilete, mappe] = imread(bilde2);
125         DDbilete2 = double(bilete);
126
127         figure(15) %************* Line in annulus: Defined ...
                above ***********************    FIGUR 15  ...
                *************************
128         %Analyse along chosen line down along annulus from ...
                top to bottom
129         for ix=annxtop:annxbot
130             ylin = annytop + fix(DYann*(ix-annxtop)/DXann);
131             %             fargeannR(iy)= ...
                    bilete(iy,xlin,1); % uint8
132             %             fargeannG(iy)= bilete(iy,xlin,2);
133             %             fargeannB(iy)= bilete(iy,xlin,3);
134             fargeannR2(ix)= DDbilete2(ylin,ix,1); % Double ...
                    precision
135             fargeannG2(ix)= DDbilete2(ylin,ix,2);
136             fargeannB2(ix)= DDbilete2(ylin,ix,3);
137         end
138
139         fargediff2=abs(fargeannB2-fargeannR2);
140         % Difflager2=fargediff2;
141         fargesum2=(fargeannR2+fargeannG2+fargeannB2)/3;
142         Difflager2=fargesum2; %fargeannB;
143         plot(Difflager1,'k')
144         % Difflager1 defined previously at line 256 ...
                (figure 3) and line 300 for figure(4)
145         hold on
146         % mappe = 'Bilde: 3.3.3 splittet\'
147         %title([mappe navn2])
```

```
148         title(['File name = ' files(nn).name ' - no ...
                averaging'])
149         xlabel('Pixel position along vertical line in ...
                annulus')
150         ylabel('Relative B-R pixel intensity along ...
                vertical annulus line')
151         plot(Difflager2,'b')
152         legend('black is first "reference" image', 'blue ...
                is consecutive images','Location', 'northwest')
153         hold off
154
155
156         figure(17) ...
                %****************************************** ...
                   FIGUR17  ************************
157         % ************************************************
158         % Nf x Mf punkts midling av farge intensitet
159         % Nf og Mf definerer bredde (y) og lengde (x) av ...
                et utsnitt av
160         % bildet rundt iy og xlin som velges ut
161         % ************************************************
162
163         for ix=annxtop:annxbot
164             ylin = annytop + fix(DYann*(ix-annxtop)/DXann);
165             NabomidlingR4 = ...
                    DDbilete2(ylin-Nf:ylin+Nf,ix-Mf:ix+Mf,1);
166             NabomidlingG4 = ...
                    DDbilete2(ylin-Nf:ylin+Nf,ix-Mf:ix+Mf,2);
167             NabomidlingB4 = ...
                    DDbilete2(ylin-Nf:ylin+Nf,ix-Mf:ix+Mf,3);
168
169             fargeannR4(ix) = mean(NabomidlingR4,'all');
170             fargeannG4(ix) = mean(NabomidlingG4,'all');
171             fargeannB4(ix) = mean(NabomidlingB4,'all');
172         end
173         fargediff4=abs(fargeannB4-fargeannR4);
174         % Difflager4=fargediff4;
175         fargesum4=(fargeannR4+fargeannG4+fargeannB4)/3;
176         Difflager4=fargesum4; %fargeannB;
177         plot(Difflager1,'k') %
178         hold on
179         title(['File name = ' files(nn).name ' - ' ...
                int2str(Nf*2+1) 'transverse width x' ...
                int2str(Mf*2+1) ' axial vertical point average'])
180         %title(['Bilde: 0 mlps At 0,01 1.run KLIPPET\' ...
                navn2 ' - ' int2str(Nf*2+1) 'x' ...
                int2str(Mf*2+1) ' point average'])
181         xlabel('Pixel position along vertical line in ...
                annulus')
```

```
182         ylabel('Relative B-R pixel intensity - running ...
                average')
183         plot(Difflager4,'r')
184         legend('black is first "reference" image', 'red is ...
                consecutive images')
185         hold off
186         %
187         % ************************************************
188         figure(18) % Show image and figure 15 in one ...
                ************************************ ...
                ***************  figure(18) ...
                ****************************
189         % ************************************************
190         FIL = ['File name: 3.3.3 splittet - ' files(nn).name]
191         sgtitle(['Analysis of images.  ' FIL])
192
193         subplot(3,1,1)
194         imshow(bilde2)
195         title(['Measurement along red line in annulus: ...
                (x,y)_{top} = ('...
196             num2str(annxtop) ',' num2str(annytop) '), ...
                    (x,y)_{bottom} = (' ...
197             num2str(annxbot) ',' num2str(annybot) ').' ...
                    newline ...
198             'Image interleave factor = '  ...
                    num2str(Hoppover) ])
199         annxline = [annxtop annxbot];
200         annyline = [annytop annybot];
201         DXann = annxbot-annxtop
202         DYann = annybot-annytop
203
204         %        num2str(annxbot) ') ,' num2str(annybot) ...
                ')' newline
205         %        'Image interleave factor = ' ...
                num2str(Hoppover)] )
206         hold on
207         axis('image')
208         plot(annxline,annyline,'-r')
209         % http://matlab.izmiran.ru/help/techdoc ...
210         %/creating_plots/axes_pr7.html
211         % set(gcf,'CurrentAxes',h)
212         % annotation('textbox',[.1 .1 .1 ...
                .2],'String','Text outside the ...
                axes','EdgeColor','none')
213         hold off
214
215         % *****************
216         subplot(3,1,2)
```

```
217         plot(Difflager1,'k') % Difflager1 defined at line ...
                256 (figure 3)
218         hold on
219         title(['Image pixel analysis (as in fig15) - File ...
                name: 3.3.3 splittet ' files(nn).name])
220         xlabel('Pixel position along vertical line in pipe ...
                annulus')
221         %ylabel('Relative B-R pixel intensity along ...
                vertical annulus line')
222         ylabel('Total pixel intensity along vertical ...
                annulus line')
223         plot(Difflager2,'b') % Difflager2 fra figur 15
224         plot(Difflager4,'r') % Difflager4 fra figur 17
225         text(100,80,['Image length scale =  ' ...
                num2str(round(xlengdeskala)) ' pixels/cm'])
226         legend('black is first "reference" image', 'blue: ...
                non-averaged pixel values','red is same as ...
                below','Location', 'northwest')
227         hold off
228
229         % ******************
230         subplot(3,1,3)
231         plot(Difflager1,'k') % Difflager1 defined at line ...
                256 (figure 3)
232         hold on
233         % title(['File name = ' files(nn).name ' - no ...
                averaging'])
234         title([' Cross section pixel averaged (transverse ...
                x axial) ' int2str(Nf*2+1) 'x' int2str(Mf*2+1) ...
                ' as in fig17)'])
235         xlabel('Pixel position along (axial) vertical line ...
                in annulus')
236         ylabel('Total pixel (R+G+B) intensity')
237         plot(Difflager4,'r') % Difflager4 fra figur 17
238         legend('black is first "reference" image', 'red: ...
                image by image transverse averaged pixel ...
                values','Location', 'northwest')
239         hold off
240
241         hold off
242     end
243 end
```

[27]

Appendix D

Pasco measurements

Pressure and volt measurements to monitor the fluid column height and flow velocities respectively. Example is from run 3.3.3:

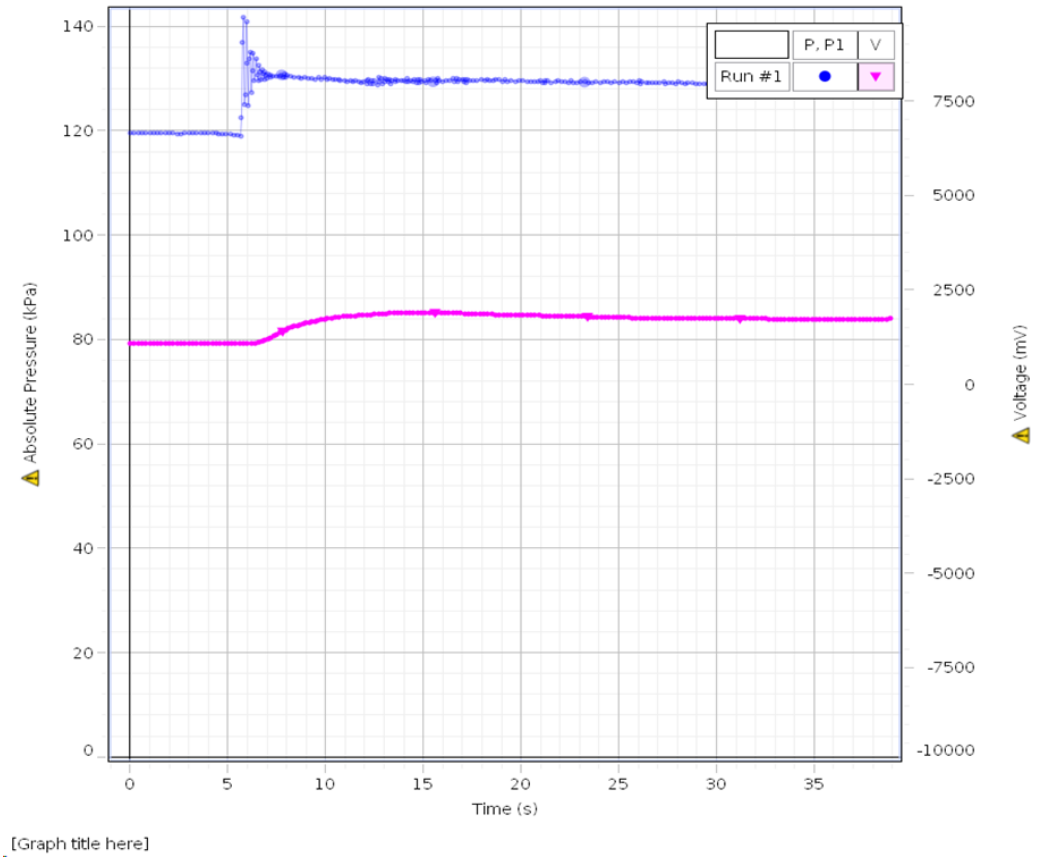

Figure D.1: Pasco measurements for 3.3.3

Appendix E

Photographs of the experimental setup

Figure E.1: Setup before improvements showing camera and fish tank

Figure E.2: Improved setup showing curtains, fish tank, and camera stand

Figure E.3: Top view of curtain and curtain frame

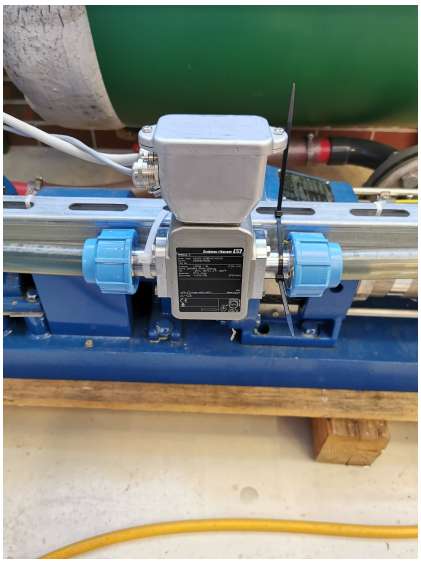

Figure E.4: Flow meter

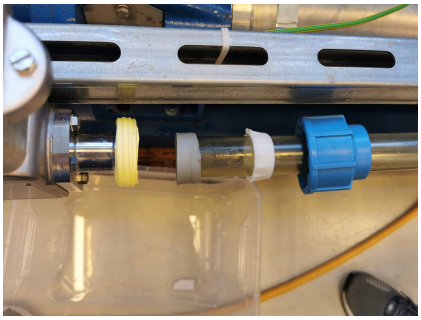

Figure E.5: Flow meter coupling

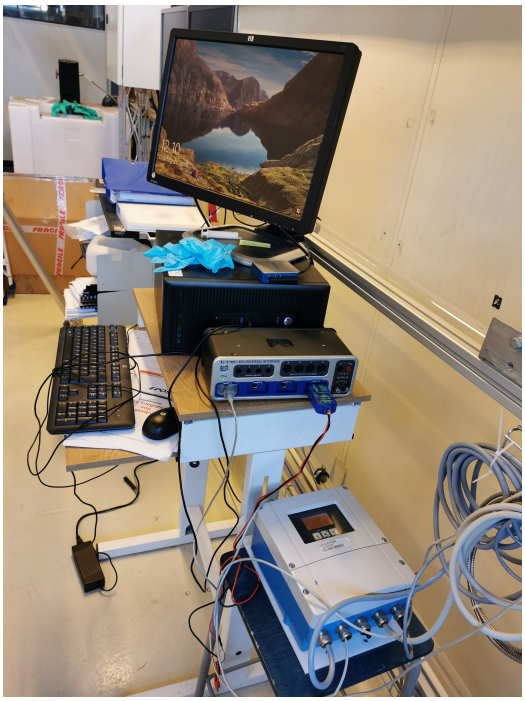

Figure E.6: Computer, PASCO interface and flow meter display

Figure E.7: PASCO absolute pressure sensor and tube coupling for the presure sensor

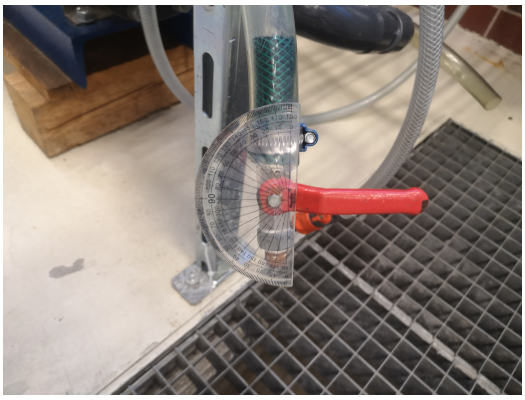

Figure E.8: Outlet valve with protractor

Figure E.9: Y-coupling for overflow

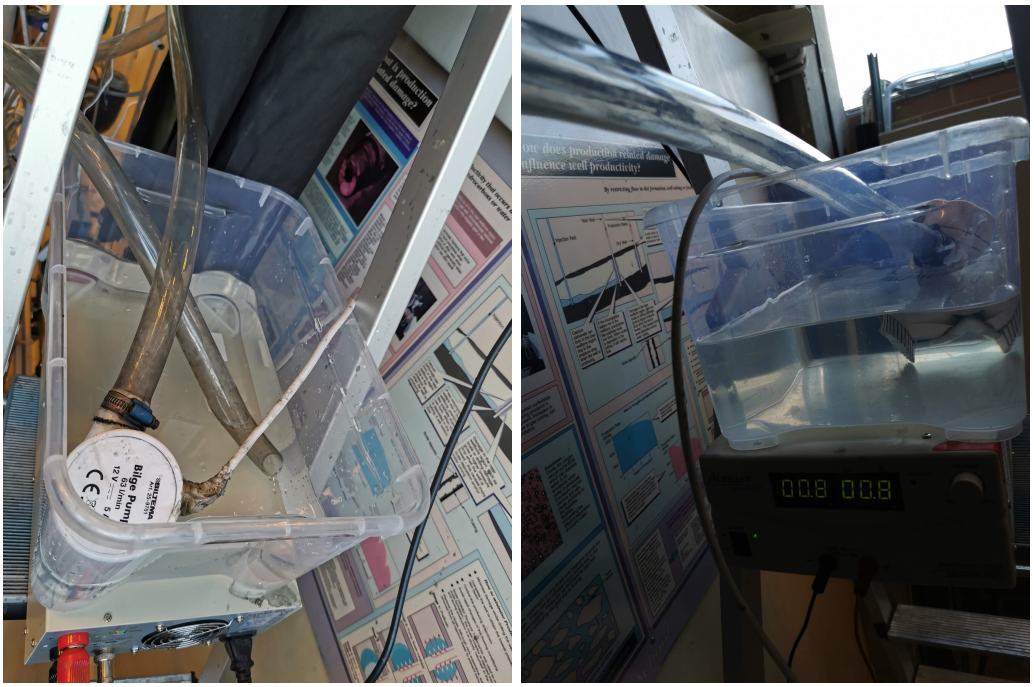

Figure E.10: Pump, tank and power supply

Figure E.11: LED-strip used for illumination